Advanced high temperature heat pump configurations using low GWP refrigerants for industrial waste heat recovery: A comprehensive study

Carlos Mateu-Royo[a*], Cordin Arpagaus[b], Adrián Mota-Babiloni[a], Joaquín Navarro-Esbrí[a], Stefan S. Bertsch[b]

[a] ISTENER Research Group, Department of Mechanical Engineering and Construction, Universitat Jaume I, Campus de Riu Sec s/n, E12071 Castelló de la Plana, Spain

[b] Eastern Switzerland University of Applied Sciences, Institute for Energy Systems, Werdenbergstrasse 4, 9471 Buchs, Switzerland

Abstract

High temperature heat pumps (HTHPs) have a great potential to improve industrial processes with thermal demand through industrial waste heat recovery and revalorization. Vapor compression HTHPs are very sensitive to the cycle configuration, refrigerant, components, and operating temperatures. This study compares eight advanced cycle configurations and nine low global warming potential (GWP) refrigerants from an energetic, economic, and environmental comprehensive perspective to illustrate an optimum selection for different HTHP applications. Firstly, several single-stage and two-stage compression cycles are proposed adding different components, such as the ejector, economizer, parallel compressor, flash tank, or additional evaporators and condensers. Moreover, an internal heat exchanger (IHX) has been included in all configurations to maximize the energy performance and ensure dry compression. Secondly, HC-601, HC-600, HC-600a, HFO-1336mzz(Z), HFO-1336mzz(E), R-514A, HCFO-1233zd(E), HCFO-1224yd(Z), and HFO-1234ze(Z) are considered as alternative low GWP refrigerants to replace the hydrofluorocarbon HFC-245fa. The results indicate that a two-stage cascade becomes the most appropriate configuration for high temperature lifts (60K and above). In contrast, single-stage cycles with economizer and parallel compression are suitable for low temperature lifts (50 K and below). HCFO-1233zd(E) and HCFO-1224yd(Z) show a trade-off between coefficient of performance (COP) and volumetric heating capacity (VHC). Advanced HTHPs configurations can save up to 68% of the equivalent CO_2 emissions compared to a natural gas boiler.

Keywords: Hydrofluoroolefines (HFO); Refrigerant; Vapor Compression Systems; Energy Efficiency; Total Equivalent Warming Impact (TEWI), Waste Heat Utilization

Nomenclature

COP	coefficient of performance (-)
E_a	annual energy consumption (kWh)
h	specific enthalpy (kJ kg^{-1})
$\dot{m}$	refrigerant mass flow rate (kg s^{-1})
n	lifespan of the vapour compression system (years)
L	annual refrigerant leakage rate (kg year^{-1})
P	pressure (MPa)
$\dot{Q}$	thermal loads (kW)
T	temperature (ºC)

* Corresponding author: Carlos Mateu-Royo
Tel: +34 964 728 134
Email: mateuc@uji.es

u	velocity (m s^{-1})
r_p	pressure ratio (-)
s	specific entropy (kJ kg^{-1} K^{-1})
v	specific volume (m^3 kg^{-1})
$\dot{W}$	electric power consumption (kW)
VHC	volumetric heating capacity (kJ m^{-3})

Greek symbols

α	recycling factor of the refrigerant
β	indirect emission factor ($kgCO_{2\text{-eq.}}$ kWh^{-1})
δ	heat source ratio (-)
ρ	density (kg m^{-3})
ε	effectiveness (-)
η	efficiency (-)
Δ	variation

Subscripts

ad	adiabatic
c	compressor
cond	condensation
crit	critical
d	diffuser
disch	discharge
e	ejector
eco	economizer
em	electromechanical
evap	evaporation
ev	expansion valve
in	inlet
i	intermediate
is	isentropic
k	condenser
liq	liquid
m	mixing chamber
n	nozzle
o	evaporator
out	outlet
p	primary
pp	pinch point
r	refrigerant
ref	reference
s	secondary
SC	sub-cooling
SH	superheat
sink	heat sink
suc	suction
source	heat source
vap	vapour
vol	volumetric

Abbreviations

EES	engineering equation solver
GWP	global warming potential
HC	hydrocarbon

HCFO	hydrochlorofluoroolefin
HFC	hydrofluorocarbon
HFO	hydrofluoroolefin
HS	high stage
HTHP	High temperature heat pump
IHX	internal heat exchanger
LS	low stage
NBP	normal boiling point
ODP	ozone depletion potential
PC	parallel compression
SS	single-stage
TEWI	total equivalent warming impact
TS	two-stage

1. Introduction

In the coming years, industrial high temperature heat pumps (HTHP) are expected to increasingly replace fuel-driven boilers for the generation of steam, hot water, and hot air, among others [1,2]. In fact, HTHPs are a technology with a considerable potential for waste heat recovery and the reduction of CO_2 emissions, using renewable electricity as driven energy and being integrated into trigeneration systems to provide heat, cold, and electricity [3].

It is proved that the range of commercial HTHPs has grown steadily in recent years. Arpagaus et al. [2] identified more than 26 HTHP products from 15 manufacturers on the market, providing heat supply temperatures from 90 °C to a maximum of 165 °C (e.g., Viking's HeatBooster HBS4 and Kobelco's SGH 120/165). Thus, various industrial processes such as drying, pasteurization, sterilization, steam generation, papermaking, food preparation, and heat recovery could benefit from the introduction of HTHPs.

Based on EU-28 data, Kosmadakis [4] estimated that industrial HTHPs could cover approximately 28 TWh per year of thermal requirements from 100 to 150 °C, which corresponded to about 1.5% of the total heat consumption. The necessary waste heat to be recovered was about 21 TWh per year, which was 7% of the total waste heat potential in the EU industries. At the European level, the most promising sectors were identified as non-metallic minerals, food, paper, and non-ferrous metal.

The type of refrigerant (also referred to as working fluid) and thermodynamic cycle configuration have a decisive influence on the design of industrial HTHPs. Among others, the refrigerant has to be suitable for the operating conditions (e.g., adequate temperatures and pressures), energy efficient, commercially available, and above all, future-proof and environmentally friendly (according to F-gas regulations). As a result, it must have a low Global Warming Potential (GWP) and a zero or negligible Ozone Depletion Potential (ODP). Besides, the critical temperature needs to be high enough to allow subcritical cycle condensation, which is often required in industries.

In practice, the hydrofluorocarbon HFC-245fa is the dominant refrigerant used in industrial HTHPs [2]. However, its GWP value is 858 and is likely to be phased out (or down) in the coming years. Natural refrigerants and synthetic hydrofluoroolefins (HFOs) and hydrochlorofluoroolefins (HCFOs) are considered as the 4th generation of low GWP refrigerants that are expected to replace HFCs [5]. The main alternatives to HFC-245fa in HTHP and Organic Rankine Cycle (ORC) applications are HFO-1366mzz(Z), HFO-1234ze(Z), HCFO-1233zd(E), HCFO-1224yd(Z), as well as the hydrocarbons HC-601 (n-Pentane) and HC-600 (n-Butane). Although HCFOs are chlorinated, their ODP is barely negligible due to their short

lifetime in the atmosphere [6,7]. Moreover, there are national regulations like the Swiss *ChemRVV* [8], which allow the use of refrigerants with an ODP below 0.0005.

Among the HFO refrigerants, HFO-1336mmz(Z) offers the highest critical temperature, 171.3 °C, at a relatively low pressure (29 bar). This refrigerant is non-flammable (safety group A1), has zero ODP, a GWP of 2, and an atmospheric life of 22 days. According to Kontomaris [9], it is stable up to 250 °C and, therefore, suitable for applications such as waste heat recovery, organig Rankine cycle (ORC), and steam generation. Its isomer, HFO-1336mzz(E), has a GWP of approximately 18, a critical temperature of 137.7 °C, and higher volumetric heating capacity (VHC) [10]. Relatively little information is available on HFO-1234ze(Z) [11–14], which is considered mildly flammable, but difficult to ignite (safety group A2L, burning velocity lower than 10 cm s^{-1}).

A characteristic feature of some of the aforementioned refrigerants is a positive slope (dT/ds > 0) of the saturated vapor curve. Thus, a minimum vapor suction superheating is often required to ensure dry compression. A cycle designed with an internal heat exchanger (IHX) (also known as a liquid-to-suction heat exchanger) appears to be the most convenient option. Several studies in different vapor compression applications demonstrated that a single-stage cycle with an IHX is energy efficient for low-temperature lifts up to 40 K [2,9,10,15–20]. However, as the temperature lift rises, two-stage cycles become more convenient. For example, an optimized two-stage cascade with IHX is recommended for temperature lifts from 60 to 70 K or even higher [15,21].

Table 1 summarises the current studies that theoretically investigated the energy efficiency of low GWP refrigerants in different HTHP cycle configurations. Indeed, the number of publications has been notably increased in the last five years, indicating that HTHPs is an emerging research topic. Energy efficiency improvements are achieved in particular by the introduction of an IHX, ejector, expander, and two-stage and multi-stage extraction cycles. In the following, the main findings of these studies are briefly summarised.

Table 1. Summary of published theoretical studies evaluating natural and synthetic HFO/HCFO refrigerants in different HTHP cycles (SS: single-stage, TS: two-stage, eco: economizer).

Refrigerants															**Cycle Configurations**										
HFO-1336mzz(Z)	**HCFO-1233zd(E)**	**HCFO-1224yd(Z)**	**HFO-1234ze(Z)**	**HFO-1234ze(E)**	**HFO-1336mzz(E)**	HFO-1234yf	**R-514A**	HFC-365mfc	**HFC-245fa**	**HC-601 (n-pentane)**	**HC-600 (n-butane)**	HC-290 (propane)	R-717 (ammonia)	R-718 (water)	Basic cycle	**SS with IHX**	**SS ejector/expansion with IHX**	**SS with eco and parallel comp.**	Two SS with IHX in parallel	TS with IHX	**TS with economizer and IHX**	**TS with economizer and IH**	**TS with flash tank and IHX**	**TS extraction**	TS cascade extraction	**TS cascade with IHX**	Triple tandem with IHX	Three-stage with flash tanks	Three-stage extraction	**Literature Reference**
	✓		✓	✓				✓	✓						✓									✓					✓	[11,12]
	✓		✓	✓				✓	✓															✓	✓		✓		✓	[11]
✓				✓	✓	✓			✓						✓															[9,10]
✓																✓														[16]
			✓												✓						✓							✓		[14]
✓	✓	✓		✓		✓				✓	✓	✓														✓				[21]
✓	✓								✓							✓				✓										[19]
✓	✓		✓	✓				✓	✓	✓	✓		✓	✓	✓															[20]
✓	✓	✓	✓	✓				✓	✓							✓														[2]
✓	✓	✓	✓	✓		✓		✓	✓							✓					✓		✓			✓				[15]
✓	✓	✓							✓						✓	✓														[22]

											✓	✓	✓	✓	✓								✓			✓	[1]
✓	✓	✓	✓					✓			✓		✓		✓												[18]
			✓						✓		✓				✓	✓	✓										[23]
	✓	✓							✓														✓				[24]
	✓		✓	✓				✓		✓	✓	✓	✓		✓											✓	[25]
✓			✓						✓	✓	✓			✓	✓												[26]
✓	✓	✓	✓	✓					✓		✓				✓		✓										[27]
✓	✓	✓	✓			✓	✓		✓	✓	✓	✓			✓												[28]
✓	✓	✓	✓				✓		✓							✓			✓					✓			[29]
✓	✓	✓	✓	✓	✓		✓		✓	✓	✓					✓	✓	✓			✓	✓	✓	✓		✓	**This study**

Bamigbetan et al. [20] evaluated the performance of several hydrocarbons (HC-600, HC-600a, HC-601, HC-601a) and HFO-1234ze(E), HFO-1234ze(Z), HCFO-1233zd(E), HFO-1336mzz(E), HFO-1336mzz(Z)) concerning their suitability in a basic HTHP up to 125 °C heat production. HC-600 and HCFO-1233zd(E) showed the highest potential for immediate future implementation. Mainly, HC-600 could be directly used in compressors already developed for HC-600a and HC-290 with minor modifications. Another comprehensive screening of Frate et al. [18] proves that HCFO-1233zd(E) reaches the best compromise between COP and VHC.

Luo and Zou [23] simulated advanced single-stage cycles using HC-600, HC-600a, HFO-1234ze(Z), and HFC-245fa at a condensing temperature 120 °C and a temperature lift of 40 K. Expander and ejector-expansion cycles reduced the expansion losses and improved cycle energy efficiency from 10 to 18% and from 8 to 14% compared to a basic cycle using HFC-245fa, respectively. HFC-245fa, HC-600 and HFO-1234ze(Z) showed similar COPs, while HC-600a COP was from 4% to 14% lower than that of HFC-245fa.

In particular, water (R-718) has received increasing attention in recent years in the HTHP field. Wu et al. [26] compared the performance of R-718, HC-600, HC-601, HFO-1234ze(Z), HFO-1336mzz(Z), and HFC-245fa in a basic cycle. The simulations showed that R-718 has the best system performance and Carnot efficiency above 120 °C condensation temperature and 70 K temperature lift. On the other hand, a compressor with a larger volume flow is required, and discharge temperatures above 200 °C would need a special intercooler design for safe operation. Bergamini et al. [1] investigated the natural refrigerants HC-290, HC-600a, R-717, and R-718 in two-stage HTHP cycles. From a thermodynamic perspective, HTHPs were competitive to natural gas boilers for heat production up to 180 °C with temperature lifts of up to 160 K. R-717 was the most efficient fluid for a heat source and sink temperatures of below 60 °C and 110 °C, respectively. At the same time, R-718 performed better at a higher temperature. Moreover, a two-stage cycle with a flash tank and R-717/R-718 cascade configuration achieved the highest COPs.

Mikielewicz and Wajs [25] identified ethanol (HFC-152a) as a working fluid with the highest COP in a single-stage cycle from 130 °C to 150 °C condensing temperature and 80 K lift. However, the VHC is the smallest of all fluids analyzed, which renders a significantly larger compressor size and consequently implies a higher acquisition cost of the component. Additionally, two-stage cascade systems with HC-601 and HFC-365mfc in the upper stage were also examined and combined with several low GWP working fluids. HFC-365mfc/HFO-1234ze(Z) and HC-601/HFO-1234ze(Z) pairs offered the best COPs.

Simulations of Mateu-Royo et al. [19] in two-stage cycles and heat sink temperatures of up to 150 °C showed the highest COP using HC-601, followed by HFO-1336mzz(Z) and HCFO-1233zd(E). Mota-Babiloni et al. [21] presented a theoretical study of a two-stage cascade using HCFO-1233zd(E), HCFO-1224yd(Z), HFO-1336mzz(Z) and HC-601 in the high-stage and HFO-1234yf, HFO-1234ze(E), HC-600, HC-600a and HC-290 in the low-stage. The highest efficiency was reached with the refrigerant pair HC-601/HC-600. Regarding HFO refrigerants (low or non-flammable), the combination of HFO-1336mzz(Z)/HFO-1234ze(E)

achieved the highest COP, whereas HFO-1224yd(Z)/HFO-1234yf showed the lowest efficiency among the investigated refrigerants.

The VHC is a critical parameter for the compressor design as it determines its size and cost. Arpagaus et al. [30] also conducted thermodynamic analyses of two-stage cycles with economizer and flash tank, and cascade configurations. They concluded that a trade-off between COP and VHC needs to be found when selecting refrigerants. HFO-1336mzz(Z) achieved the highest COP of all HFO and HCFO investigated from 120 to 160 °C in all cycles. Each refrigerant achieved an optimal COP at a heat sink temperature of about 30 K below the critical temperature. HFO-1336mzz(Z) was proposed as a replacement for HFC-365mfc, while HCFO-1233zd(E), HCFO-1224yd(Z), and HFO-1234ze(Z) were closer to HFC-245fa in terms of COP and VHC [2,15].

Mateu-Royo et al. [22] simulated a single-stage HTHP cycle with IHX at condensing temperatures from 115 to 145 °C and evaporating temperatures from 45 to 75 °C. Compared to HFC-245fa, HCFO-1233zd(E), HFO-1336mzz(Z) and HCFO-1224yd(Z) improved the COP by 27%, 21% and 17%, respectively. HCFO-1233zd(E) and HCFO-1224yd(Z) had a comparable suction volumetric flow rate to HFC-245fa, while HFO-1336mzz(Z) had an 80% lower value, indicating that it would be required a much larger compressor and installation size. The Total Equivalent Warming Impact (TEWI) metric showed a reduction in CO_2 equivalent emissions from 59% to 61% with the low GWP refrigerants compared to HFC-245fa.

Alhamid et al. [24] investigated HCFO-1224yd(Z) and HCFO-1233zd(E) in a two-stage cycle with flash tank at 110 °C condensation and 50 to 70 °C evaporation supplied by solar thermal energy. Both HCFO refrigerants showed comparable performance to HFC-245fa and minor CO_2 emissions. The highest exergy destruction was found in the compressor, followed by the condenser, expansion valve, and evaporator. Hu et al. [14] analyzed two-stage and three-stage compression systems with HFO-1234ze(Z) for waste heat recovery in industrial processes up to 120 °C. Compared to a single-stage cycle, the COP improvements were between about 9% and 15%.

HTHPs for high temperature glides at the heat sink, and high temperature lifts from source to sink require more complex cycle designs. Kondou and Koyama [31] explored different multi-stage and cascade cycles for upgrading waste heat from 80 to 160 °C and a temperature glide at the sink of 90 K. The efficiencies of HFC-365mfc, HFO-1234ze(E), and HFO-1234ze(Z) were compared. A three-stage extraction cycle with HFO-1234ze(Z) achieved the highest efficiency thanks to reduced exergy losses in the expansion valve and the condenser. A two-stage cascade cycle with HFC-365mfc/HFO-1234ze(Z) also provided high COP and practical benefits in compressor control and lubricant selection. Fukuda et al. [11] examined, in particular, a two-stage extraction cycle, in which two compressors are connected in series, and the heat sink is divided into two condensers. Specifically, this configuration is an advantage at high sink temperature glides and high pressure ratios.

Recently, Diewald et al. [29] compared such a two-stage extraction cycle with a parallel IHX cycle achieving high temperature glides on the heat sink with 70 °C inlet and from 100 °C to 160 °C outlet. HFO-1234ze(Z), HFO-1336mzz(Z), R-514A, HCFO-1233zd(E) and HCFO-1224yd(Z) were analysed. At 130 °C heat sink temperature, the COP of the two-stage extraction and the parallel IHX cycle improved around 2.5% and 7.8% compared to a single-stage IHX cycle, respectively. HCFO-1233zd(E) offered a wide range of comparable COP reaching heat sink temperatures of up to 160 °C, and higher VHC than HFO-1336mzz(Z) and R-514A. In the parallel IHX cycle, the refrigerant combination HFO-1336mzz(Z)/R-514A provided the highest COP.

In addition to the discussed cycle configurations, ejectors can be implemented along with an IHX to obtain advanced configurations. Zhang et al. [32] reviewed several ejector

configurations and showed the operational and energetic benefits, however mostly for refrigeration applications using R-744. Bai et al. [27] analyzed two ejector cycles suitable for HTHP application and investigated various low GWP refrigerants. Compared with a basic IHX cycle, the system COP of the ejector cycles could be improved by up to 14.5% by recovering expansion work (at 105 °C condensation and 30 °C evaporation temperature). HCFO-1233zd(E) yielded the highest system COP and exergy efficiency in comparison with HC-600, HCFO-1224yd(Z), HFO-1234ze(Z).

Another option for advanced cycle design is parallel compression, for which part of the refrigerant leaving the condenser is expanded to an intermediate pressure and then enters in a second compressor. Such a cycle allows a lower pressure ratio, which reduces the input power and size of the compressor. In addition, parallel compression has the advantage of reducing the refrigerant mass flow to be compressed by the main compressor. Such cycles are mainly used in transcritical R-744 heat pumps [33–36]. Based on the above discussion, ejector and parallel compression configurations are promising designs for HTHPs as alternatives to single-stage cycles.

Based on the above described, a comparative performance analysis of the most suitable cycle configurations and refrigerants covering a wide range of operating conditions is still considered as a research gap. Therefore, the purpose of this paper is to provide a comprehensive assessment of the most promising advanced configurations analysis and low GWP refrigerants for HTHPs based on COP, VHC, the environmental impact (through TEWI calculation), and economic. The eight most promising configurations and nine potential alternatives refrigerants have been selected, based on the literature review. The rest of the paper are structured as follows. Section 2 describes the selected cycle configurations and low GWP refrigerants. Section 3 introduces the methodology, modelling details, equations required, and assumptions for the energy, environmental and economic analysis. Section 4 presents the main results obtained in this theoretical study. Finally, Section 5 contains the most relevant conclusions. The results of this study aim providing provide guidelines for the further design and development of HTHPs.

2. System description

2.1. Advanced cycle configurations

As a consequence of the previous literature review, eight advanced cycle configurations have been selected to examine their potential in a wide range of operating HTHP conditions. All these configurations include an IHX to ensure a dry compression along to improve the system performance. The schematic and pressure-enthalpy (P-h) diagrams of the cycle configurations are included in Figure 1.

- Single-stage cycle (SS+IHX), reference for low temperature lifts. It is composed by a compressor, condenser, evaporator, expansion valve, and internal heat exchanger.

- Single-stage cycle with economizer and parallel compression (SS Economizer + PC). An additional compressor (parallel compressor, PC) and economizer are added. A fraction of subcooled liquid becomes evaporated and superheated by the economizer and introduced in the PC to be discharged in the condenser inlet. The compressed vapour of the PC is mixed with the discharged vapour of the main compressor before entering the condenser.

- Single-stage cycle with ejector (SS Ejector). An ejector is used to reduce the irreversibility of the expansion device, combining the currents of the evaporator outlet and the subcooled liquid. The irreversibility decrease improves the performance of the

system. A liquid tank is connected at the outlet of the ejector and brings saturated vapour to the IHX inlet, and saturated liquid to expand for the evaporator.

- Two-stage cycle cascade (TS Cascade). Two basic cycles with IHX are connected by a cascade heat exchanger, operating as the evaporator for the high-stage (HS) cycle and condenser in the low-stage (LS) cycle. Different refrigerants can be used in each stage.

- Two-stage cycle with economizer (TS Economizer), reference for high temperature lifts. This configuration separates the compression in two steps with two compressors in series, reducing the pressure ratio of each component and, therefore, increasing the energy efficiency. In the intermediate compression process, the superheated vapour from the economizer is injected. This phenomenon reduces the discharge temperature of the high stage (HS) compressor. This cycle is widely used in the industry, being already used, for example, in the commercial HTHPs of Ochsner (Austria) [2].

- Two-stage cycle with flash tank (TS Flash Tank). Similarly, this configuration divides the compression process into two compressors along with the vapour injection in the intermediate process. However, this cycle uses a flash tank instead of a closed economizer, injecting saturated vapour instead of being superheated.

- Two-stage booster cycle (TS Booster). This configuration is similar to two-stage with economizer but includes an evaporator between this component and the suction HS compressor. The additional evaporator allows waste heat recovery from two heat sources with different temperature levels.

- Two-stage extraction cycle (TS Extraction). The condensation process in this configuration is divided into two condensers that operate at different pressure conditions. This provides a significant benefit to processes with a high temperature glide between the inlet and outlet temperature of the secondary thermal fluid on the heat sink.

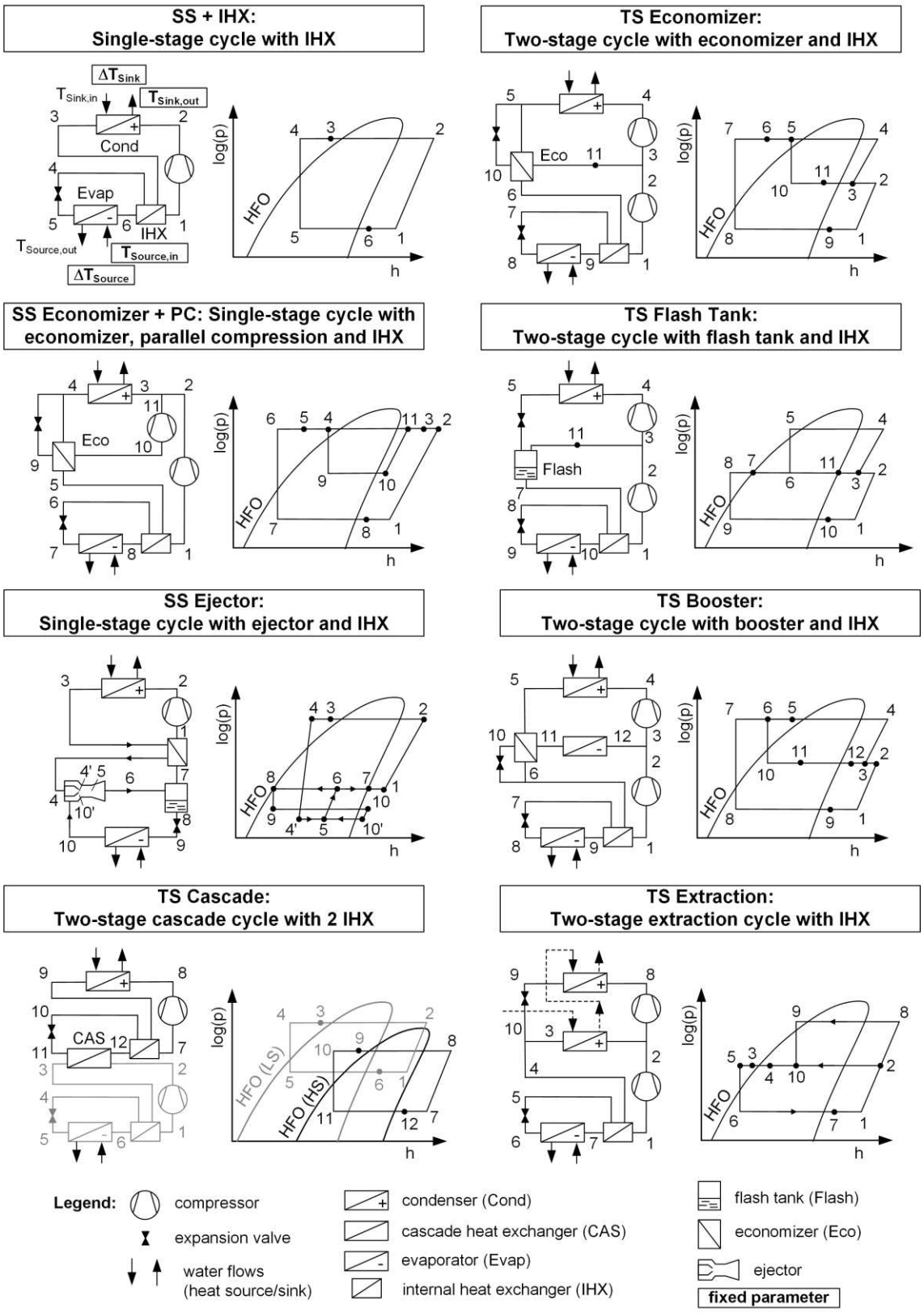

Fig. 1. Schematic representations and P-h diagrams of the advanced HTHP cycle configurations.

2.2. Low GWP refrigerants

Environmental, operational, and energetic aspects have been prioritized to select the most promising low GWP refrigerants in HTHP systems. HFC-245fa is widely used as a working fluid in HTHPs, but due to its high GWP, it should be replaced. Thus, this refrigerant is set as

the reference working fluid. The selected refrigerants have comparable thermophysical properties, as shown in Table 1. The information has been retrieved using Engineering Equation Solver (EES) [37] as the refrigerant database. It is worth to highlight that all the selected refrigerants have lower toxicity (ASHRAE class A) except for R-514A and the reference fluid HFC-245fa (ASHRAE safety class B1). Concerning flammability, all the HCs are included in the higher flammability group (A3).

In contrast, HFOs and HCFOs present no flame propagation (A1), apart from HFO-1234ze(E) that is considered as a lower flammability fluid (A2L). Regarding the ODP, all the refrigerants have a zero ODP except for the HCFOs, which presents an almost zero ODP value allowed by current national environmental regulations. Among the low GWP alternatives selected, R-514A and HFO-1336mzz(E) stand out for their novelty.

Table 2. Thermophysical properties of the selected low GWP refrigerants and HFC-245fa [37].

Refrigerant	**T_{crit} (ºC)**	**P_{crit} (MPa)**	**Vapour density (kg m^{-3})[a]**	**NBP (ºC)**	**Molecular weight (g mol^{-1})**	**ODP**	**GWP_{100}**	**ASHRAE Safety Class** [38]
HC-601	196.6	3.37	8.9	36.1	72.2	0	5	A3
R514A	178.0	3.52	22.8	29.1	139.6	0	2	B1
HFO-1336mzz(Z)	171.4	2.90	24.1	33.4	164.1	0	2	A1
HCFO-1233zd(E)	166.5	3.62	30.7	18.3	130.5	0.00034	1	A1
HCFO-1224yd(Z)	155.5	3.33	40.2	14.6	148.5	0.00012	<1	A1
HC-600	152.0	3.80	22.5	-0.5	58.1	0	4	A3
HFO-1234ze(Z)	150.1	3.53	37.2	9.8	114.0	0	<1	A2L
HFO-1336mzz(E)	137.7	3.15	62.3	7.5	164.1	0	18	A1
HC-600a	134.6	3.60	31.8	-11.7	58.12	0	20	A3
HFC-245fa (Ref.)	154.0	3.65	38.7	15.1	134.0	0	858	B1

[a] At saturated pressure of 75 °C.

Fig. 2 presents T-s and P-h diagrams of selected refrigerants. Through these diagrams, the difference in critical pressure, latent heat of vaporization and condensation, and saturation slope can be observed. Most of the alternative low GWP refrigerants present similar two-phase region than the reference fluid HFC-245fa apart from the hydrocarbons. Moreover, the critical temperature of the alternative candidates become equal or even higher in most of the refrigerants, illustrating a potential performance improvement compared to HFC-245fa.

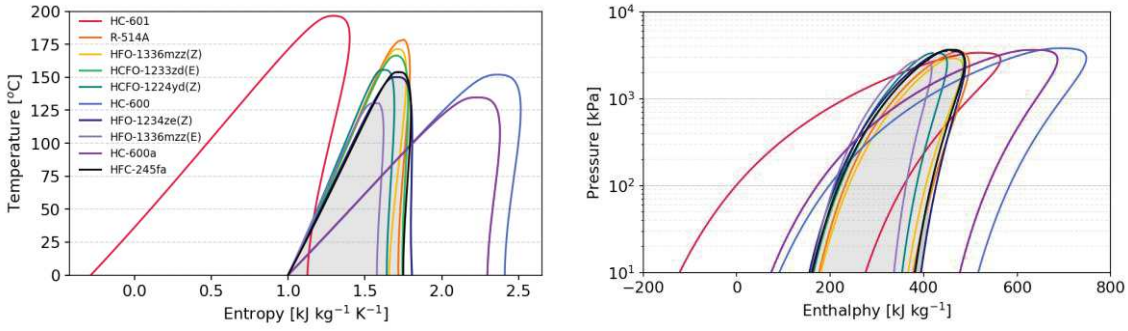

(a) (b)

Fig. 2. Thermodynamic diagrams of the alternative low GWP refrigerants and reference fluid HFC-245fa: a) T-s and b) P-h.

3. Methodology and modelling details

3.1. Methodology

The simulation results of the advanced configurations are based on the methodology presented in Fig. 3. Each cycle configuration and refrigerant, along with the boundary conditions and assumptions, are used as input parameters for the model. This model is developed using the software Engineering Equation Solver (EES, V10.6) [37], working together with REFPROP 10.0 [39]. While EES solves the thermodynamic equations of each configuration and the IHX optimization, REFPROP provides the thermophysical properties of each refrigerant. The IHX optimization, based on the Golden Section Search algorithm implemented in EES, maximizes the COP of each configuration and refrigerant, varying the IHX effectiveness without exceeding the maximum discharge temperature of each compressor, depending on the configuration. Finally, the parameters that determine the performance of the systems become the outputs, which are compared with the reference configuration (TS Economizer).

The TS cascade cycle requires the optimization of the effectiveness for both IHXs along with the intermediate condensing temperature. This is performed by the Conjugate Direction optimization method, also implemented in EES. Moreover, HFO-1336mzz(E) is not included in the EES refrigerant database, and therefore, the EES numerical models and REFPROP 10.0 have been linked.

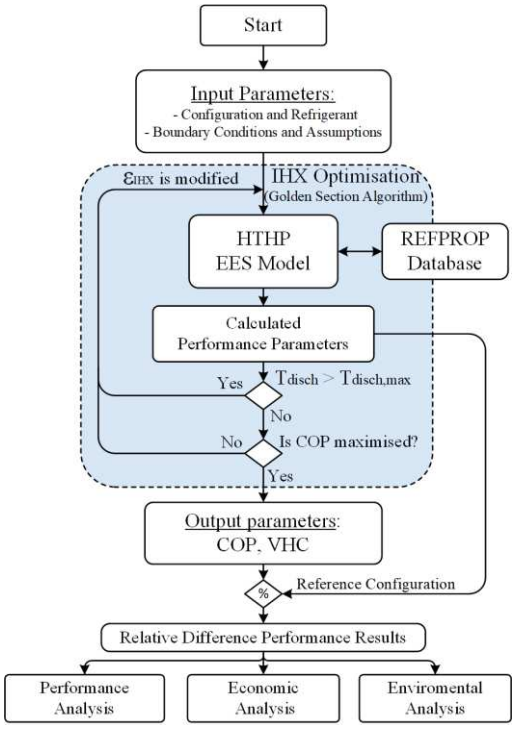

Fig. 3. Methodology flow diagram.

3.2. Boundary conditions and assumptions

The heat sink outlet temperature $T_{sink,out}$ (heat production) and heat source inlet temperature $T_{source,in}$ (e.g. waste heat) are used as operating parameters to simulate different conditions with each configuration and refrigerant. The expansion valve process is considered isenthalpic, and pressure drops along with the heat transfer to the surroundings are neglected. Table 3 presents the assumed values of the boundary conditions and the reference values.

Table 3. Assumptions and boundary conditions used in modelling simulation

Parameter	Assumed value
Heat sink outlet temperature ($T_{sink,out}$)	100 – 150 ºC (Ref. 130 ºC)
Heat source inlet temperature ($T_{source,in}$)	30 – 90 ºC

Temperature lift (ΔT_{Lift})	30 – 80 K (Ref. 60 K)
Superheat degree (ΔT_{SH})	5 K
Sub-cooling degree (ΔT_{SC})	2 K
Condenser approach temperature ($\Delta T_{pp,sink}$)	2.5 K
Evaporator approach temperature ($\Delta T_{pp,source}$)	2.5 K
Heat sink temperature glide (ΔT_{sink})	10 K
Heat source temperature glide (ΔT_{source})	10 K

In order to evaluate different waste heat sources, two different scenarios are proposed for high and low heat source temperatures. For the high heat source temperature scenario, waste heat of 70 to 90 ºC are considered based on combined heat and power (CHP) systems [40]. For the low heat source temperature scenario, waste heat between 30 to 50 ºC represent district heating networks as heat sources to upgrade the low temperature heat to industrial process heat levels [28,41].

3.3. Modelling details

This section presents and explains the numerical equations used in the modelling process of each cycle configuration. Most of the system components are common in all configurations, whereas others are specific. Thus, the essential components are firstly described, followed by the particularities in the modelling for each configuration.

One of the main components of the selected configurations is the compressor. The compressor model proposed by Winandy et al. [42], Cuevas et al. [43] and, Lemort [44] has been adapted using Eq. (1).

$$\eta_{OverUnder} = \frac{h_{disch,is} - h_{suc}}{(h_{ad} - h_{suc}) + v_{ad}(P_{disch} - P_{ad})} \quad (1)$$

This model considers the over-under compression phenomena and provides a rigorous approximation to the overall compressor efficiency in a wide range of operating conditions and refrigerants. A built-in volume ratio of 2.45 is considered, and the electro-mechanical compressor efficiency becomes proportional to the pressure ratio (r_p), Eq. (2). The proposed compressor model has been validated using manufacturer data of a commercial compressor.

$$\eta_{vol} = 1.0455 - 0.0184\, r_p - 0.0011\, {r_p}^2 \quad (2)$$

The discharge temperature T_{disch} was limited to 175 ºC in the simulation due to the thermal stability of some refrigerants operating at high temperatures [22]. The discharge temperature is highly influenced by the IHX effectiveness ε_{IHX} and therefore, this paremeter is limited. The IHX is modelled using the effectiveness method, Eq. (3).

$$\varepsilon_{IHX} = \frac{h_{vap,out} - h_{vap,in}}{h_{vap,out} - h_{liq,in}} \quad (3)$$

The economizer is a type of sub-cooler where part of the refrigerant is evaporated at higher evaporation temperatures than the main evaporator, whereas substantially subcooling the remaining refrigerant flow [45]. The mass flow injection fraction is defined as the ratio between the mass flow rate through the evaporator and the mass flow injected to the parallel (HS) compressor. A constant injection fraction of 30% is assumed for all configurations with economizer. The specific modelling equations of each configuration are described below.

3.4. Single-stage

The heating capacity $\dot{Q}_k$ and the compressor power consumption $\dot{W}_c$ are obtained using Eq. (4) and Eq. (5). Finally, the COP and VHC are calculated using Eq. (6) and Eq. (7).

$$\dot{Q}_k = \dot{m}\,(h_3 - h_2) \tag{4}$$

$$\dot{W}_c = \frac{\dot{m}\,(h_{2,is} - h_1)}{\eta_{OverUnder}\,\eta_{em}} \tag{5}$$

$$COP = \frac{h_3 - h_2}{h_{2,is} - h_1}\eta_{OverUnder}\,\eta_{em} \tag{6}$$

$$VHC = \rho_1 \eta_{vol}(h_3 - h_2) \tag{7}$$

3.5. Single-stage cycle with economizer and parallel compression

The intermediate pressure is calculated considering a temperature approach of 5 K between the liquid economizer outlet and saturated temperature of the expanded liquid fraction. Moreover, the superheating degree of the vapor at the economizer outlet is 5 K. The energy and mass balance of the different refrigerant mass flow rates is obtained with Eq. (8) and (9), respectively.

$$\dot{m}_{\text{total}}\, h_3 = \dot{m}\, h_2 + \dot{m}_{PC}\, h_{11} \tag{8}$$

$$\dot{m}_{\text{total}} = \dot{m} + \dot{m}_{PC} \tag{9}$$

Finally, the performance parameters of this cycle are calculated based on Eq. (10) to (13).

$$\dot{Q}_k = \dot{m}_{total}(h_3 - h_2) \tag{10}$$

$$\dot{W}_c = \frac{\dot{m}\,(h_{2,is} - h_1)}{\eta_{OverUnder}\,\eta_{em}} + \frac{\dot{m}_{PC}\,(h_{11,is} - h_{10})}{\eta_{OverUnder,PC}\,\eta_{em,PC}} \tag{11}$$

$$COP = \frac{\dot{m}_{total}(h_3 - h_2)}{\frac{\dot{m}\,(h_{2,is} - h_1)}{\eta_{OverUnder}\,\eta_{em}} + \frac{\dot{m}_{PC}\,(h_{11,is} - h_{10})}{\eta_{OverUnder,PC}\,\eta_{em,PC}}} \tag{12}$$

$$VHC = \frac{\dot{m}_{total}(h_3 - h_2)}{\frac{\dot{m}}{\rho_1\,\eta_{vol}} + \frac{\dot{m}_{PC}}{\rho_{10}\,\eta_{vol,PC}}} \tag{13}$$

3.6. Single-stage cycle with ejector

A constant-pressure mixing model is adopted for the ejector [27,46,47], with the following assumptions:

- The ejector efficiencies are considered constant at 0.8.
- The mixing process pressure is assumed constant, complying with energy and momentum conservation.
- The kinetic energy through the ejector is neglected.
- The ejector is adiabatic.

The mass flow rate ratio between the secondary and primary fluid determines the entrainment ratio μ , which is used to evaluate the mass entrainment capacity of the ejector, Eq. (14)

$$\mu = \frac{\dot{m}_s}{\dot{m}_p} \tag{14}$$

The pressure ratio r_p is used to evaluate the pressure rise of the ejector, which is defined by the ratio between the ejector outlet (diffuser) (P_o) and secondary inlet fluid pressure (P_I), Eq. (15).

$$r_{p,e} = \frac{P_I}{P_o} \tag{15}$$

The ejector model is based on the mass, energy, and momentum conservation in the working process of the ejector components (nozzle, mixing chamber, and diffuser). The inlet velocity of the primary flow is neglected, as previously stated in the assumptions. The isentropic nozzle efficiency η_n is used to obtain the outlet velocity of the primary fluid based on energy conservation, Eq. (16).

$$u_4' = \sqrt{2\,\eta_n\,(h_4 - h_{4,is})} \tag{16}$$

The mixing efficiency η_m considers energy losses caused by the flow friction and two-phase shock in the mixing process. Hence, the mixing velocity u_5 can be obtained from momentum conservation, Eq. (17).

$$u_5 = \frac{u_4'}{1+\mu}\,\sqrt{\eta_m} \tag{17}$$

Inlet and outlet specific enthalpies of the mixed fluid can be calculated applying energy conservation in the diffuser section, Eq. (18) and (19).

$$h_5 = h_6 - \frac{1}{2}\,(u_5)^2 \tag{18}$$

$$h_6 = \frac{h_4 + \mu\,h_{10}}{1+\mu} \tag{19}$$

The isentropic diffuser efficiency η_d is used to obtain the ideal specific enthalpy at the diffuser outlet, Eq. (20).

$$h_{6,is} = h_5 + \eta_d(h_6 - h_5) \tag{20}$$

The intermediate pressure of the ejector outlet P_I can be determined with Eq. (21). Therefore, ejector outlet state parameters, including temperature, pressure, and quality, can be calculated.

$$P_I = f(h_{6,is}\,, s_{6,is}) \tag{21}$$

Finally, the performance parameters of the ejector cycle are calculated based on the following Eq. (22) to (25).

$$\dot{Q}_k = \dot{m}_p(h_3 - h_2) \tag{22}$$

$$\dot{W}_c = \frac{\dot{m}_p\,(h_{2,is} - h_1)}{\eta_{OverUnder}\,\eta_{em}} \tag{23}$$

$$COP = \frac{h_3 - h_2}{h_{2,is} - h_1} \eta_{OverUnder}\, \eta_{em} \tag{24}$$

$$VHC = \rho_1 \eta_{vol} (h_3 - h_2) \tag{25}$$

3.7. Two-stage cycle cascade

For the two-stage cascade system, a difference of 3 K between the LS condensing temperature and HS evaporation temperature is assumed in the intermediate heat exchanger. The condensation temperature in the intermediate heat exchanger and the IHX effectiveness are optimized to maximize the COP without exceeding the maximum discharge temperature. The performance parameters of this configuration are based on Eq. (26) to (29).

$$\dot{Q}_k = \dot{m}_{HS}(h_9 - h_8) \tag{26}$$

$$\dot{W}_c = \frac{\dot{m}_{HS}\,(h_{8,is} - h_7)}{\eta_{OverUnder,HS}\,\eta_{em,HS}} + \frac{\dot{m}_{LS}\,(h_{2,is} - h_1)}{\eta_{OverUnder,LS}\,\eta_{em,LS}} \tag{27}$$

$$COP = \frac{\dot{m}_{HS}(h_9 - h_8)}{\frac{\dot{m}_{HS}\,(h_{8,is} - h_7)}{\eta_{OverUnder,HS}\,\eta_{em,HS}} + \frac{\dot{m}_{LS}\,(h_{2,is} - h_1)}{\eta_{OverUnder,LS}\,\eta_{em,LS}}} \tag{28}$$

$$VHC = \frac{\dot{m}_{HS}(h_9 - h_8)}{\frac{\dot{m}_{HS}}{\rho_7\,\eta_{vol,HS}} + \frac{\dot{m}_{LS}}{\rho_1\,\eta_{vol,LS}}} \tag{29}$$

3.8. Two-stage cycle with economizer and flash tank

The two-stage cycle with economizer and two-stage cycle with flash tank use almost the same modelling equations. The only difference is that while the injected vapour becomes superheated in the economizer cycle, for the flash tank cycle is saturated. Both configurations require a method to determine the intermediate pressure, which is calculated with Eq. (30).

$$P_I = \sqrt{P_k\, P_o} \tag{30}$$

For these configurations, two mass flow rates are mixed in the suction of the HS compressor, and therefore, the energy and mass balance of the different refrigerant mass flow rates is obtained with Eq. (31) and (32), respectively.

$$\dot{m}_{\text{total}}\, h_3 = \dot{m}\, h_2 + \dot{m}_{ECO}\, h_{11} \tag{31}$$

$$\dot{m}_{\text{total}} = \dot{m} + \dot{m}_{ECO} \tag{32}$$

Finally, the performance parameters of those configurations are calculated based on the following equations:

$$\dot{Q}_k = \dot{m}_{total}(h_5 - h_4) \tag{33}$$

$$\dot{W}_c = \frac{\dot{m}_{total}\,(h_{4,is} - h_3)}{\eta_{OverUnder,HS}\,\eta_{em,HS}} + \frac{\dot{m}\,(h_{2,is} - h_1)}{\eta_{OverUnder,LS}\,\eta_{em,LS}} \tag{34}$$

$$COP = \frac{\dot{m}_{total}(h_5 - h_4)}{\frac{\dot{m}_{total}\,(h_{4,is} - h_3)}{\eta_{OverUnder,HS}\,\eta_{em,HS}} + \frac{\dot{m}\,(h_{2,is} - h_1)}{\eta_{OverUnder,LS}\,\eta_{em,LS}}} \tag{35}$$

$$VHC = \frac{\dot{m}_{total}(h_5 - h_4)}{\frac{\dot{m}_{total}}{\rho_3\,\eta_{vol,HS}} + \frac{\dot{m}}{\rho_1\,\eta_{vol,LS}}} \tag{36}$$

3.9. Two-stage booster cycle

Equations used for this configuration are similar to two-stage with economizer and flash tank cycles with the difference that the intermediate pressure P_I is fixed by the evaporation temperature of the additional evaporator. In this case, a temperature approach of 2.5 K between the secondary fluid outlet and the evaporating temperature is assumed to calculate the intermediate evaporation pressure. The energy and mass balance of the different refrigerant mass flow rates is obtained with Eq. (37) and (32), respectively. The performance parameters of this configuration are calculated using previous equations.

$$\dot{m}_{\text{total}}\,h_3 = \dot{m}\,h_2 + \dot{m}_{ECO}\,h_{12} \tag{37}$$

3.10. Two-stage extraction cycle

The condensation process of the two-stage extraction cycle is divided into two condensers. Therefore, the condensation pressure and the intermediate pressure are calculated assuming a temperature approach of 2.5 K between the condensing temperatures and the secondary fluid outlets. Moreover, two currents coming from the condensers are mixed before the IHX. The energy and mass balance of the different refrigerant mass flow rates is through Eq. (38) and (39), respectively.

$$\dot{m}_{\text{total}}\,h_4 = \dot{m}\,h_{10} + \dot{m}_I\,h_3 \tag{38}$$

$$\dot{m}_{\text{total}} = \dot{m} + \dot{m}_I \tag{39}$$

Finally, the performance parameters of this configuration are calculated based on Eq. (40) to (43).

$$\dot{Q}_k = \dot{m}\,(h_9 - h_8) + \dot{m}_I\,(h_3 - h_2) \tag{40}$$

$$\dot{W}_c = \frac{\dot{m}\,(h_{8,is} - h_2)}{\eta_{OverUnder,HS}\,\eta_{em,HS}} + \frac{\dot{m}_{total}\,(h_{2,is} - h_1)}{\eta_{OverUnder,LS}\,\eta_{em,LS}} \tag{41}$$

$$COP = \frac{\dot{m}\,(h_9 - h_8) + \dot{m}_I\,(h_3 - h_2)}{\frac{\dot{m}\,(h_{8,is} - h_2)}{\eta_{OverUnder,HS}\,\eta_{em,HS}} + \frac{\dot{m}_{total}\,(h_{2,is} - h_1)}{\eta_{OverUnder,LS}\,\eta_{em,LS}}} \tag{42}$$

$$VHC = \frac{\dot{m}\,(h_9 - h_8) + \dot{m}_I\,(h_3 - h_2)}{\frac{\dot{m}}{\rho_2\,\eta_{vol,HS}} + \frac{\dot{m}_{total}}{\rho_1\,\eta_{vol,LS}}} \tag{43}$$

3.11. Environmental evaluation

For the environmental analysis, the Total Equivalent Warming Impact (TEWI) metric has been determined for each configuration and refrigerant to quantify the equivalent CO_2 emissions caused by refrigerant leakage (direct emissions) and energy consumption of each HTHP system (indirect emissions) [48]. The TEWI is calculated following Eq. (44).

$$TEWI = GWP \cdot L \cdot n + GWP \cdot m_r \, (1 - \alpha) + n \cdot E_a \cdot \beta \tag{44}$$

All parameters and assumptions for the TEWI analysis are presented in Table 4. HTHPs are usually contained in machinery rooms, and consequently, an annual leakage rate of 5% of the total refrigerant charge is considered [49]. Moreover, the average electricity emission factor for the European Union is used [50].

Table 4. Assumptions considered in the TEWI analysis.

Parameter	Value
Annual refrigerant leakage (L)	5 kg (5% of the total refrigerant charge)
Lifespan of the system (n)	15 years
Refrigerant charge (m_r)	100 kg
Recycling factor of the refrigerant (α)	0.7
Indirect emission factor (β)	295.8 g CO_2 kWh^{-1} [50]

4. Results and discussion

This section presents and discusses the results of the investigation. Firstly, the energy performance results of each configuration and refrigerant are evaluated for different temperature lifts. Secondly, a multi-objective analysis illustrates the trade-off between COP and VHC in order to select the optimum configuration for each proposed scenario. Then, the most optimum configurations are analyzed along with two individual applications. Finally, economic and environmental analyses complete the evaluation of configurations and refrigerants.

4.1. Performance evaluation of advanced configurations

The comparison of the energy performance is based on the COP and VHC parameters. Fig. 4 presents the results of the proposed configurations with a production temperature of 130 °C, using HFC-245fa as a working fluid.

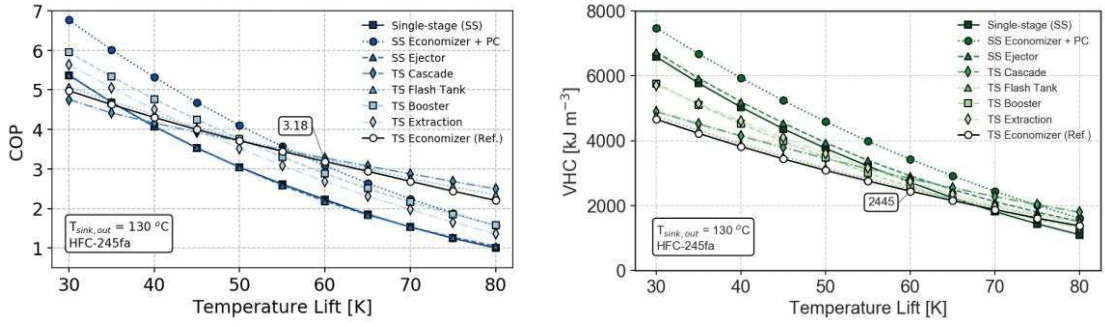

(a) (b)

Fig. 4. Performance analysis of each configuration with different temperature lifts, using HFC-245fa: a) COP and b) VHC.

At low temperature lifts, the SS Economizer + PC configuration provides the highest COP. However, an increase in the temperature lift notably affects this configuration. Particularly, above 60 K, the TS Cascade configuration remains as the most efficient one, followed by the TS Flash tank. The combination of two compressors operating with different refrigerants and the optimization of the intermediate pressure explains these results.

Regarding VHC, the SS Economizer + PC outperforms in the majority of the temperature lift range, justified by the combination of two compressors in parallel and the increase of sub-cooling produced by the Economizer. As observed for the COP, this parameter also decreases rapidly with the increase of the temperature lift. At the maximum temperature lift studied (80 K), again, the TS Cascade is the most convenient option, but in this case, the SS Economizer + PC results remain being slightly lower.

4.2. Comparison of low GWP refrigerants

After discussing the behaviour of the configurations, the effect produced by the selection of refrigerants is assessed, as presented in Fig. 5.

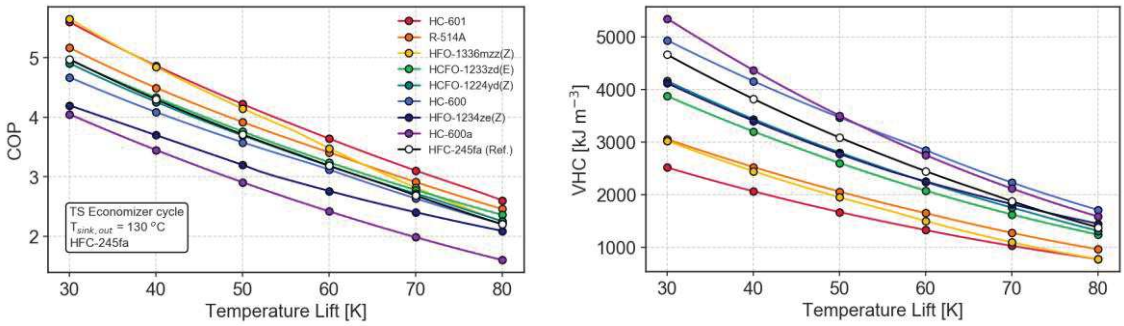

(a) (b)

Fig. 5. Performance analysis of each refrigerant in the TS Economizer (reference) at different temperature lifts: a) COP and b) VHC.

At lower temperature lifts, HFO-1336mzz(Z) and HC-601 end with the highest COP. While the COP of HFO-1336mzz(Z) considerably drops with the increase of the temperature lift, that of HC-601 has a lower reduction. This refrigerant still presents the highest energy performance at higher temperature lifts. Contrary to that concluded for the COP, the refrigerants with the highest VHC are HC-600a and HC-600, and the ones with the worst results are HC-601 and HFO-1336mzz(Z). Given the different conclusions for both parameters analyzed, a trade-off comparison would be required for obtaining the most convenient option for each application.

4.3. Performance optimization

The energetic results have been presented in the previous section at different temperature lifts. However, the performance parameters have a significant difference between each configuration and refrigerant. Thus, this section presents a multi-objective evaluation, where COP and VHC are comprehensively evaluated to select the optimum configurations and refrigerants. The performance parameters, COP and VHC, of each configuration and refrigerant are presented in Fig. 6 and 7, respectively. These figures contain the absolute values for HFC-245fa and the relative values of low GWP refrigerants respect to the reference fluid.

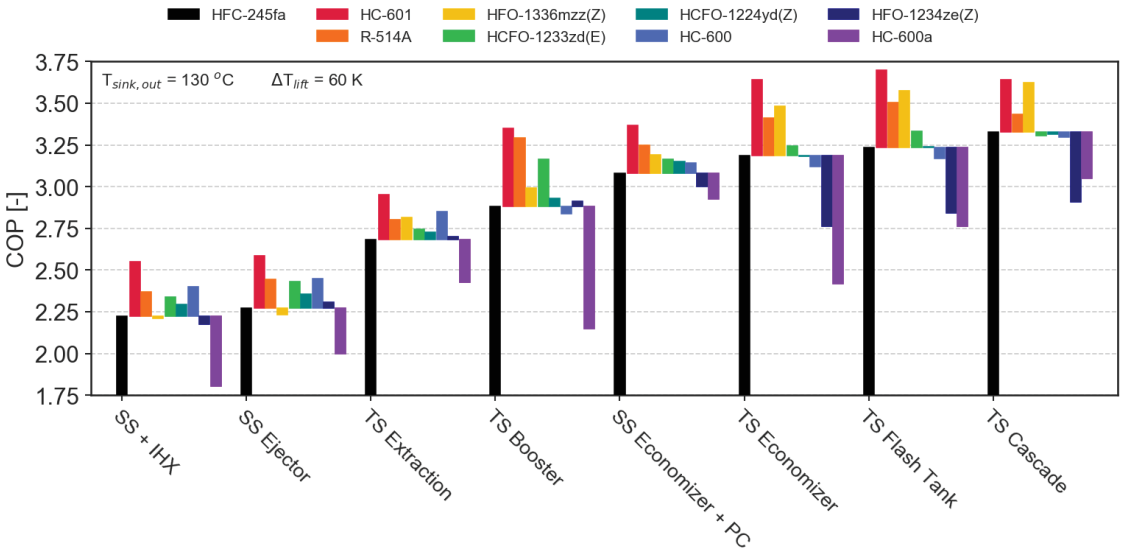

Fig. 6. COP results of each configuration and refrigerant, operating at reference conditions ($T_{sink,out}$ = 130 °C, ΔT_{Lift}=60 K).

The energy performance increases as the configuration becomes more advanced with the addition of components to the single-stage cycle. The addition of an ejector increases the COP compared to the SS + IHX between 1% and 10%, but they remain below the reference values of the TS Economizer cycle. The additional compressor causes a significant COP improvement, as the rest of the cycles illustrate. Although the TS Extraction and TS Booster are the two-stage cycles with the lowest performance improvements, these configurations are designed for special applications that will be explained in the following sections. The use of a parallel compressor in the SS Economizer + PC cycle presents a significant heating capacity increase but also shows a slight decrease in COP due to the high temperature lift. Finally, the TS Flash tank and TS Cascade present the highest performance improvements, being influenced by the possibility of operating with high IHX effectiveness values without exceeding the maximum compressor discharge temperature.

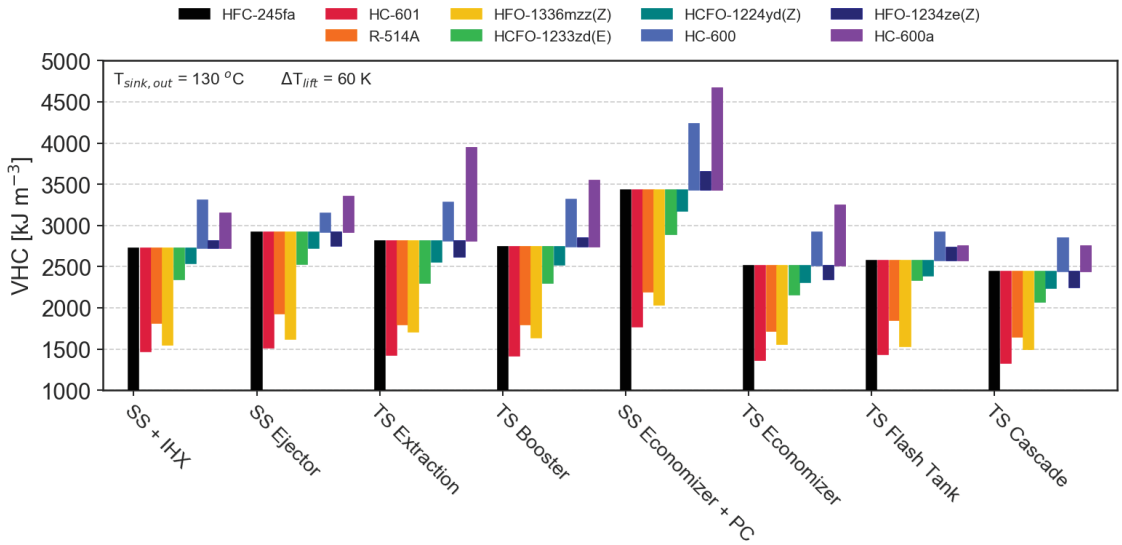

Fig. 7. VHC results of configuration and refrigerant pairs, operating in the reference conditions ($T_{sink,out}$=130 °C, ΔT_{Lift}=60 K).

Regarding the VHC evaluation, the SS Economizer + PC exhibits the highest VHC increase compared to the other proposed configurations. The fraction of the mass flow rate extracted at

the condenser outlet is compressed by a small parallel compressor that augments the suction volumetric flow rate. However, this mass flow rate extraction decreases the main compressor size, obtaining as a result a significant VHC improvement. It can be appreciated that the use of the ejector in the SS Ejector cycle reduces the compressor size, and therefore, VHC is improved. Finally, the use of two compressors in series increases the overall volumetric mass flow rate, requiring a greater compressor to provide the same heating capacity, which means that the VHC becomes reduced.

Moreover, the performance parameters have been compared using as the reference the TS Economizer (Ref.) with HFC-245fa. Fig. 8 presents the main results of this evaluation as relative COP and VHC difference for each cycle configuration and refrigerant.

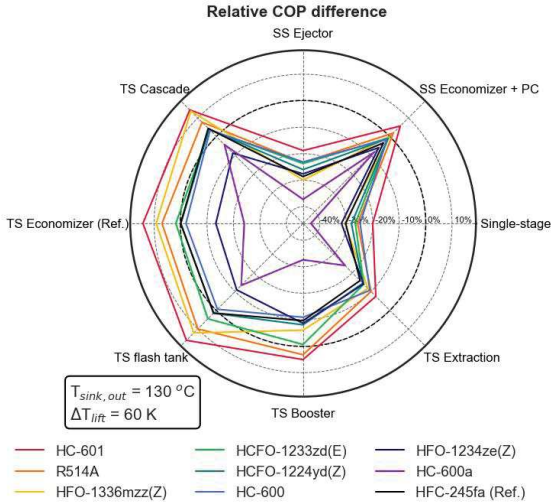

(a)

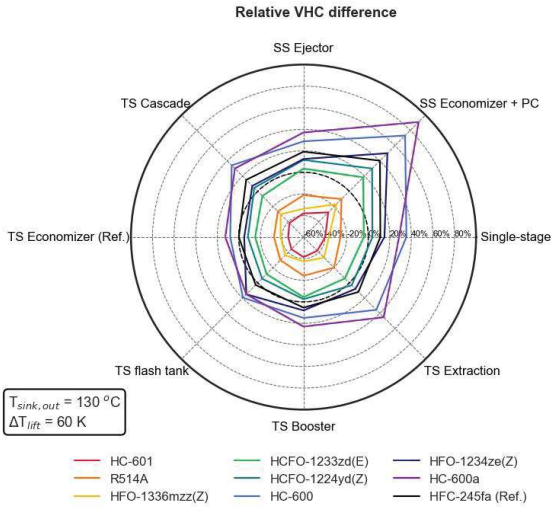

(b)

Fig. 8. Relative energy performance differences compared to the reference TS Economizer using HFC-245fa: a) COP and b) VHC

Concerning the cycle configurations, the TS Cascade and TS Flash tank exhibit the greatest COP improvements, up to 15% and 14%, respectively. These results are consistent with the conclusions obtained by Arpagaus et al. [15]. The SS Economizer + PC provides a significant COP improvement, even though this configuration does not use two compressors in series. These results are in concordance with Fang et al. [51], which concludes (in refrigeration applications) that this configuration obtains from 25% to 36% performance improvement compared to conventional systems. Diewald et al. [29] illustrate that the TS Extraction cycle

slightly improves COP. Finally, SS Ejector slightly improves the energy performance and requires more compact compressors that single-stage configurations, which is consistent with results exposed by Zhang et al. [32]. Thus, the results presented in this study are coherent with previously published studies.

About the refrigerants, HC-601 and HFO-1336mzz(Z) present the highest COP improvements in the proposed configurations but with the lowest VHC values. This is caused by their low suction density that requires a higher compressor to provide the same heating capacity than the other refrigerants. Contrary, HC-600 and HC-600a have a significant performance decrease compared with HFC-245fa but a considerable VHC improvement that allows them to use more compact compressors with these refrigerants. The other low GWP candidates show a trade-off between COP and VHC. These results are in concordance with Arpagaus et al. [30], Mateu-Royo et al. [19], and Mota-Babiloni et al. [21], which conclude that HC-601 and HFO-1336mzz(Z) provide the highest COP improvements among other refrigerants. Moreover, HC-600 and HFO-1234ze(E) in the TS Ejector have similar values than HFC-245fa, whereas HC-600a presents a COP reduction, which is consistent with Luo and Zou [23]. Finally, HCFO-1233zd(E) and HCFO-1224yd(Z) show close values to HFC-245fa, that is in concordance with several studies [17,20,25,28]. Hence, results for configurations and refrigerant pairs proposed in this work are consistent with those available in the literature.

COP and VHC are studied in the literature separately. However, both parameters need to be evaluated together in order to select the proper configuration for each application. Thus, both performance parameters are compared together with the reference TS Economizer (Ref) in different conditions, using HFC-245fa as the refrigerant. Fig. 9 exhibits the multi-objective evaluation of COP and VHC for the optimal configuration selection.

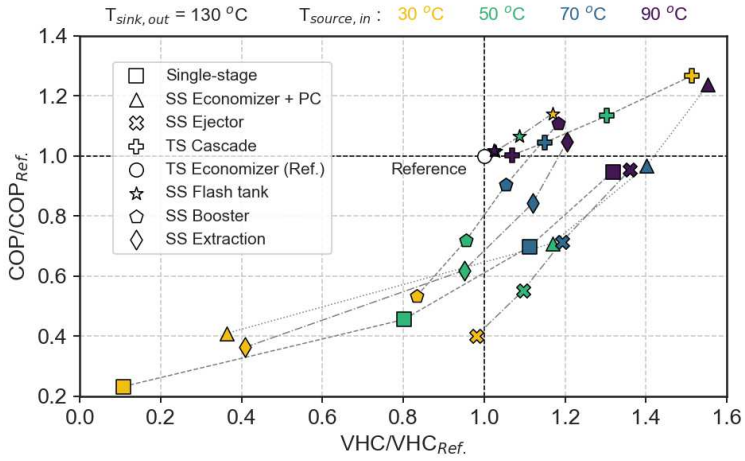

Fig. 9. Performance optimization of the proposed configurations compared with the reference TS Economizer for different applications.

For the low temperature lift scenario, corresponding to heat source temperatures between 70 ºC to 90 ºC for a heat sink temperature of 130 ºC, the SS Economizer + PC exhibits the highest COP and VHC increase compared to the reference. Therefore, this configuration would be the optimum selection at this condition. Nevertheless, it presents a substantial drop when the temperature lift increases. On the contrary, the TS Cascade presents similar COP and VHC than TS Economizer at a low temperature lift. However, as the temperature lift overcomes 60 K, the TS Cascade shows significant improvements, being the configuration with the highest COP and VHC.

4.4. Optimum Cycle Configurations

This section presents the main results of the optimum cycle configurations for low and high temperature lift scenarios using HFC-245fa as the base refrigerant. Fig. 10 exhibits the selection of the proper configuration for different combinations of heat sink and source temperatures.

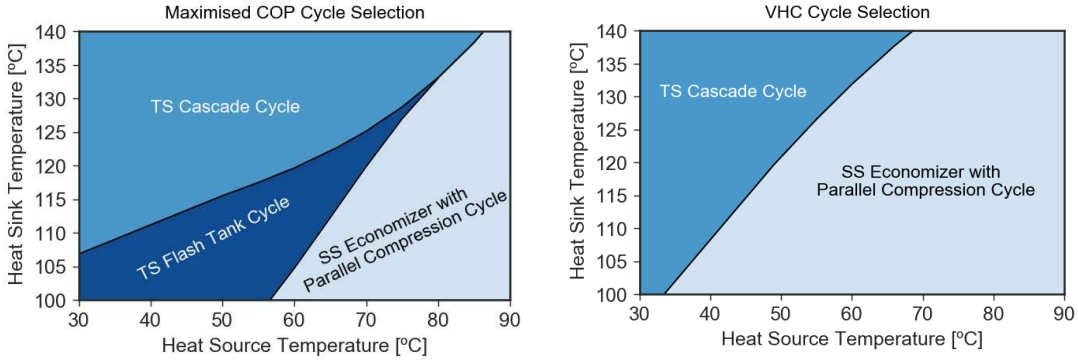

(a) (b)

Fig. 10. Optimum cycle configuration selection for different heat sink and source temperatures, using HFC-245fa as refrigerant: a) COP and b) VHC.

The TS Cascade is confirmed as the proper configuration for high temperature lifts, this is at high heat sink and low heat source temperatures. However, the TS Flash tank cycle becomes a proper cycle for low heat sink and low-medium heat source temperatures. Finally, the SS Economizer + PC exhibits the highest COP values operating at high heat source temperatures and a wide range of heat sink temperatures. The VHC comparison illustrates that the TS Cascade and the SS Economizer + PC provide the highest VHC. Therefore, both cycles are selected as the optimum for low and high heat source temperature applications, respectively.

4.4.1. Low-temperature heat source scenario

This scenario requires a high temperature lift, and the TS Cascade becomes the proper configuration to overcome thermal requirements with a valuable performance. This configuration requires the selection of the proper cascade condensing temperature, which takes place in the intermediate heat exchanger, between the HS and LS cycles. The cascade condensing temperature can be optimized to provide the maximum COP in each operating point, as shown in Fig. 11.

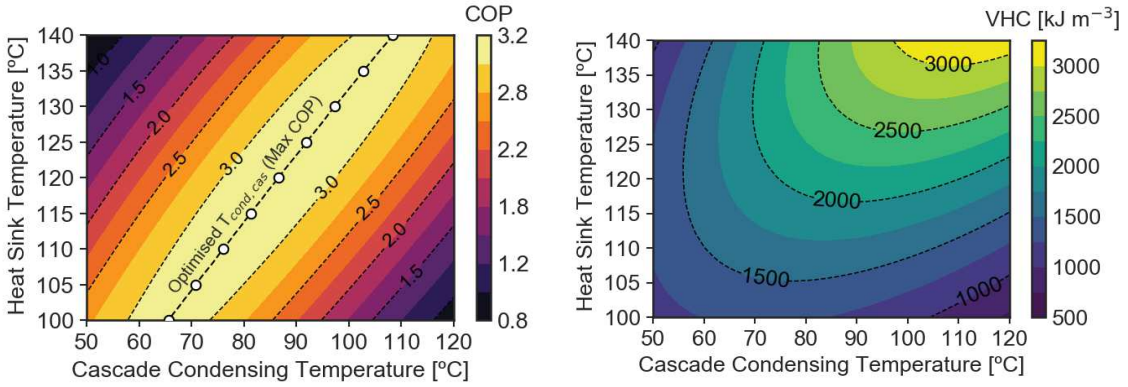

(a) (b)

Fig. 11. *Optimization of the TS Cascade cycle at different heat sink temperatures and condensing cascade temperature, operating with a low heat source temperature of 40 ºC and HFC-245fa: a) COP and b) VHC.*

Nevertheless, the optimal cascade condensing temperature does not provide the highest VHC at the same time, as illustrated in Fig. 11b. Thus, proper optimization of the cascade condensing temperature along with the IHX effectiveness of each cycle will provide the highest

performance in each condition. Moreover, the TS Cascade can be used with different refrigerant pairs in the HS and LS cycle that also require proper optimization to provide the maximum COP values.

Hence, a screening of different refrigerant pairs has been carried out to evaluate the optimal refrigerant pair in the TS Cascade cycle, analyzing COP, VHC, and the compromise between them, as shown in Fig. 12.

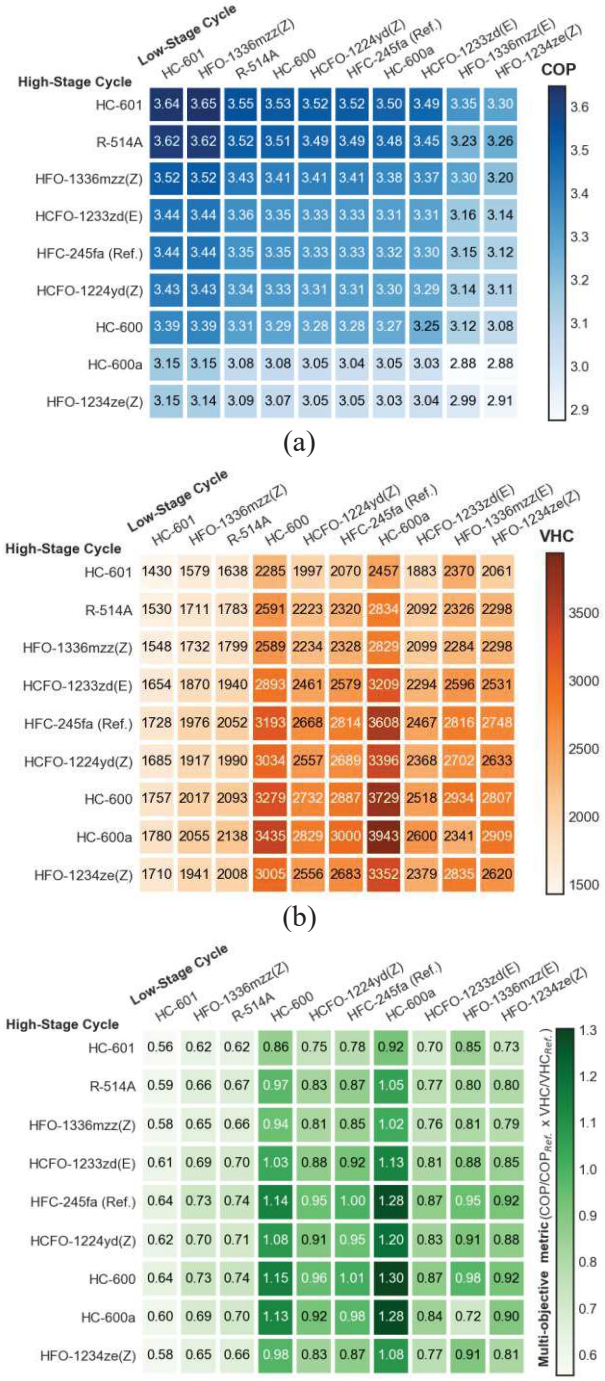

Fig. 12. Refrigerant pair selection for TS Cascade cycle, operating at heat sink temperature of 130 ºC and heat source temperature of 40 ºC: a) COP, b) VHC, and c) Multi-objective evaluation.

The refrigerant pair HC-601/HFO-1336mzz(Z) (HS and LS refrigerants, respectively) provides the highest COP, whereas HC-600a/HC-600a presents the highest VHC values and therefore,

more compact compressors and installation are expected. HC-601/HC-601 can be used as a natural refrigerant solution with similar COP values compared to the highest refrigerant pair while R-514A/HFO-1336mzz(Z) can be an HFO solution with comparable COP results. However, these refrigerant pairs have a low suction density that requires large compressor size, and therefore, the VHC of this solution becomes significantly low.

Thus, a multi-objective evaluation of COP and VHC compared to the reference cascade refrigerant pair HFC-245fa/HFC-245fa illustrates the most balanced refrigerant pair, as shown in Fig.12c. The use of HC-600a or HC-600 in the LS cycle provides higher results than the reference because the VHC increase becomes more significant than the COP improvement using HC-601, HFO-1336mzz(Z) or R-514A. However, the refrigerant pair selection will depend on different factors such as electricity price or components cost.

Fig. 13 illustrates the COP and VHC difference between the optimal cycle TS Cascade and the reference TS Economizer for different operating conditions, using HFC-245fa as the refrigerant in both cycles.

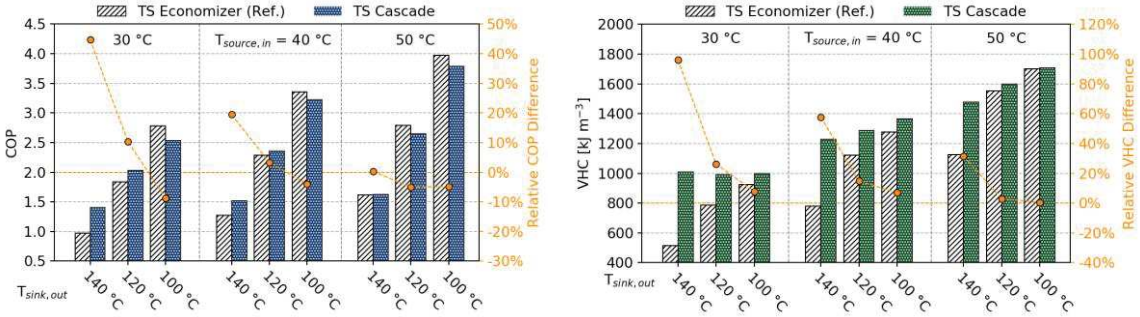

Fig. 13. Performance parameter results of the TS Cascade as low-temperature heat source solution compared to the reference TS Economizer, using HFC-245fa: a) COP and b) VHC.

As the temperature lift increases, the TS Cascade presents a higher relative COP difference than the reference cycle TS Economizer, ending with up to 48% COP improvement. A similar response is observed for the VHC, for which the relative improvement is up to 58%. However, a significant COP value higher than 1.5 is required to be economically competitive with gas boilers. These COP values are obtained operating with a temperature lift below 70 K. Thus, the TS Cascade significantly improves the performance compared with the reference TS Economizer in low-temperature heat source applications and becomes the optimal configuration to replace conventional heating system for temperature lifts up to 70 K.

4.4.2. High-temperature heat source scenario

For high temperature waste heat recovery with heat source temperatures between 70 and 90 ºC, the SS Economizer + PC becomes the most appropriate cycle configuration, as shown in Fig. 14. Different heat sink and source temperatures are proposed to evaluate the system response in different situations.

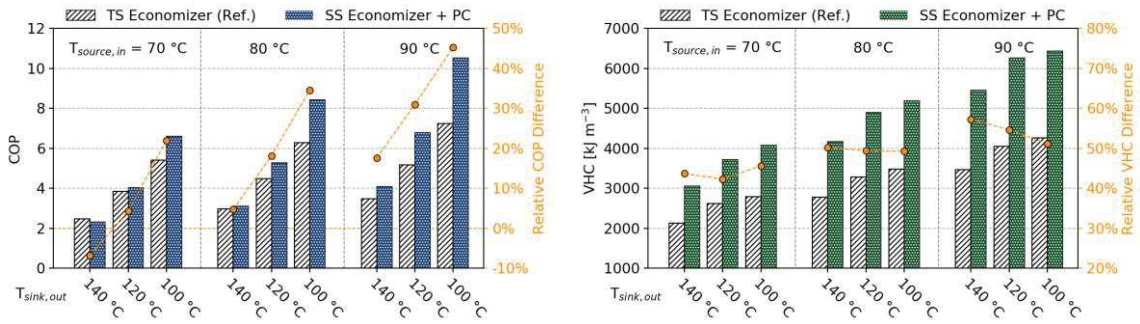

(a) *(b)*

Fig. 14. Performance parameters results of the SS Economizer + PC as high-temperature heat source solution compared to the reference TS Economizer, using HFC-245fa: a) COP and b) VHC.

Contrary to the low-temperature scenario, the SS Economizer + PC presents greater relative COP improvements as the temperature lift decreases. Thus, this configuration shows significant benefits when both heat sink and source are close. Compared to the TS Economizer, the optimal configuration obtained up to 47% COP and 58% VHC increases. Hence, the SS Economizer + PC becomes an optimal solution using high-temperature heat sources, that is the case of waste heat recovery from thermal engines.

4.5. Multi-temperature and high heat sink glide configurations

This section illustrates the potential of the TS Booster and TS Extraction cycles. Although these configurations do not present remarkable performance improvements compared to others, they are designed for special applications where they can show potential.

4.5.1. Booster compression system with economizer

The TS Booster cycle differs from other configurations because is composed by two evaporators. This fact allows recovering waste heat from two sources at different temperatures (i.e. multi-temperature heat pump). Fig. 15 illustrates the remarkable benefits of this configuration with the variation of the medium temperature heat source and heating capacity between both evaporators through the use of gamma (δ), the ratio of the heat input at the medium temperature level in relation to the total heat input. This parameter is proposed by Arpagaus et al. [36] to evaluate booster systems.

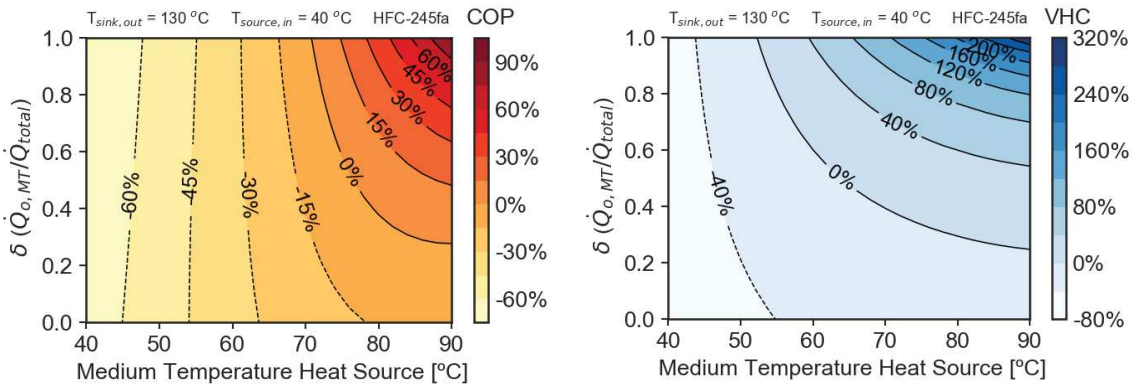

(a) *(b)*

Fig. 15. Performance parameters evaluation of the TS Booster cycle compared to the reference TS Economizer, operating with HFC-245fa: a) COP and b) VHC.

Operating at lower to medium temperature heat sources, this cycle shows notable performance drop compared to the reference cycle TS Economizer. However, TS Booster presents a COP and VHC improvement, operating at higher medium temperature heat sources. Hence, this cycle

configuration can be an optimum solution to use district heat at 40 ºC as one heat source and heat rejected from thermal engines as the other waste heat source at intermediate temperature level.

4.5.2. Two-stage extraction cycle

The condensing process of the TS Extraction cycle is divided between two condensers in series. This configuration does not present significant COP improvements compared to the reference cycle TS Economizer when considering low heat sink glides. However, this situation looks different as the operating heat sink glide increases, as shown in Fig. 16.

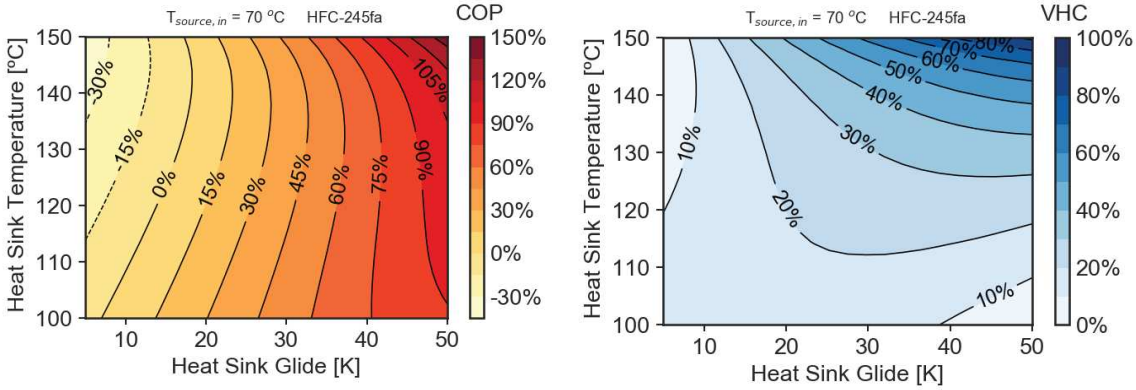

(a) (b)

Fig. 16. Performance parameters evaluation of the TS Extraction cycle compared to the reference TS Economizer, operating with HFC-245fa: a) COP and b) VHC.

The heat sink temperature glide has been fixed at 10 K for all the simulations in this study. However, some industrial processes require higher heat sink glides to overcome the thermal demands. The use of the TS Extraction cycle provides a remarkable COP and VHC improvements compared to the reference TS Economizer cycle. Thus, the TS Extraction cycle becomes the most appropriate configuration for applications that require high heat sink glide to overcome the thermal demand (e.g. in water heating applications).

4.6. Economical comparative

The cost the different cycles has been compared with the reference TS Economizer has to complete this comprehensive evaluation. The prices have been estimated from standard products of vapour compression manufacturers. The condenser heat exchanger along with the compressor, are considered sensible components of HTHP systems, and therefore, special attention has been devoted in the cost estimation. The compressors cost has been calculated as a function of the suction volumetric flow rate, using a correlation from real compressors supplier data. Finally, condenser cost has been estimated as a function of the heating capacity of each cycle. Table 5 presents the cost estimation of the selected configuration cycles and the relative cost compared to the reference TS Economizer. The number between parenthesis is the number of units of each component.

Table 5. Cost estimation of selected configuration cycles compared to the reference using HFC-245fa, for 100 kW heat source capacity.

		Single-stage	TS Extraction	TS Flash tank	SS Ejector	SS Economizer + PC	TS Economizer (Ref.)	TS Cascade	TS Booster
Components	Unit cost (€)	Cost (€) (Units number)							
HS/PC Compressor	$f(\dot{V}_{HS})$	0 (0)	2,705 (1)	5,856 (1)	0 (0)	2,120 (1)	6,605 (1)	6,264 (1)	7,049 (1)
LS Compressor	$f(\dot{V})$	15,513 (1)	13,506 (1)	9,370 (1)	14,678 (1)	13,209 (1)	11,419 (1)	9,605 (1)	10,335 (1)
Condenser	$f(\dot{Q}_k)$	6,640 (1)	5,076 (2)	5,104 (1)	5,356 (1)	5,936 (1)	5,144 (1)	5,084 (1)	5,200 (1)
Evaporator	3,500	3,500 (1)	3,500 (1)	3,500 (1)	3,500 (1)	3,500 (1)	3,500 (1)	7,000 (2)	7,000 (2)
Internal heat exchanger	1,500	1,500 (1)	1,500 (1)	1,500 (1)	1,500 (1)	1,500 (1)	1,500 (1)	3,000 (2)	1,500 (1)

Liquid-vapour separator	1,000	0 (0)	0 (0)	1,000 (1)	1,000 (1)	0 (0)	0 (0)	0 (0)	0 (0)
Economizer	1,500	0 (0)	0 (0)	0 (0)	0 (0)	1,500 (1)	1,500 (1)	0 (0)	1,500 (1)
Ejector	1,500	0 (0)	0 (0)	0 (0)	1,500 (1)	0 (0)	0 (0)	0 (0)	0 (0)
Expansion valve (electronic)	1,000	1,000 (1)	2,000 (2)	2,000 (2)	1,000 (2)	2,000 (2)	2,000 (2)	2,000 (2)	2,000 (2)
Total cost (€)		28,153	28,287	28,329	28,534	29,765	31,668	32,953	34,584
Relative Cost (%) compared to Reference		-11%	-11%	-11%	-10%	-6%	0%	+4%	+9%

Then, Fig. 17 graphically illustrates the components cost of each configuration along with the relative values. Only the TS Booster and TS Cascade overcome the initial cost of the reference configuration, TS Economizer. Therefore, in those situations in which TS Cascade is recommended, the cost of the electricity must be considered to calculate the payback period of the installation of this advanced configuration. This analysis also demonstrates that the lowest investment is not only obtained with the most basic configuration. Therefore, advanced configurations can result in similar initial costs besides providing energy performance benefits.

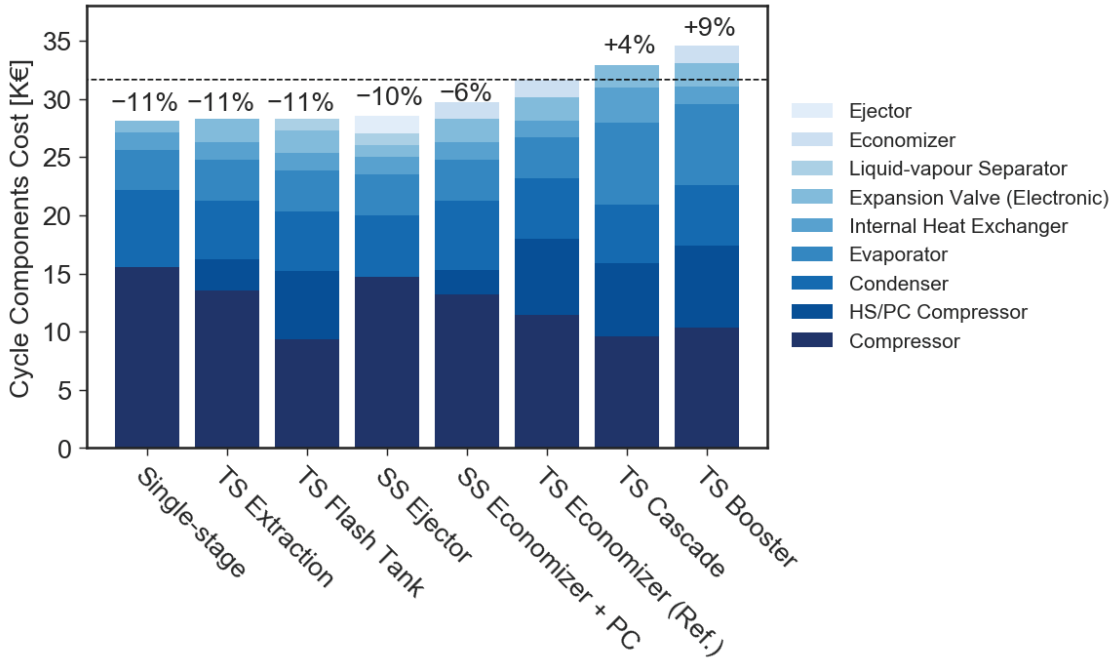

Fig 17. Economic evaluation of the proposed cycle configurations compared with the reference TS Economizer.

4.7. Environmental analysis

The Total Equivalent Warming Impact (TEWI) is calculated for the environmental comparison of the refrigerants, which in this paper focus on the carbon footprint. Fig. 18 exhibits the TEWI values of each refrigerant and proposed configuration. It can be appreciated that the TS Cascade, TS Flash Tank and, SS Economizer + PC are the cycles with the lowest equivalent CO_2 emissions due to their high energy performance compared to the other cycles.

Regarding the refrigerants, HC-601 achieves the highest equivalent CO_2 emissions reduction. However, these results are not notably different compared to HFO-1336mzz(Z) or R-514A if options with lower flammability would be required. HC-600a and HFO-1234ze(E) present a slight CO_2 emission increase compared to HFC-245fa. Since all proposed alternatives have low GWP, TEWI analysis will be determined mostly by the energy efficiency of each configuration and refrigerant pair. Thus, refrigerants with high energy efficiency will also be beneficial for the environment.

Finally, a comparison has been realized between the proposed vapour compression cycles and a natural gas boiler as conventional heating technology. An efficiency of 95% is assumed for the natural gas boiler with an emission factor of 205 g CO_2 kWh^{-1} for the natural gas [52]. The environmental results show that the HTHP system could reduce the equivalent CO_2 emission between 19% and 63% compared to conventional heating technologies. Hence, advanced HTHP configurations show a considerable potential to reduce the equivalent CO_2 emissions and, therefore, promote sustainability and climate change mitigation.

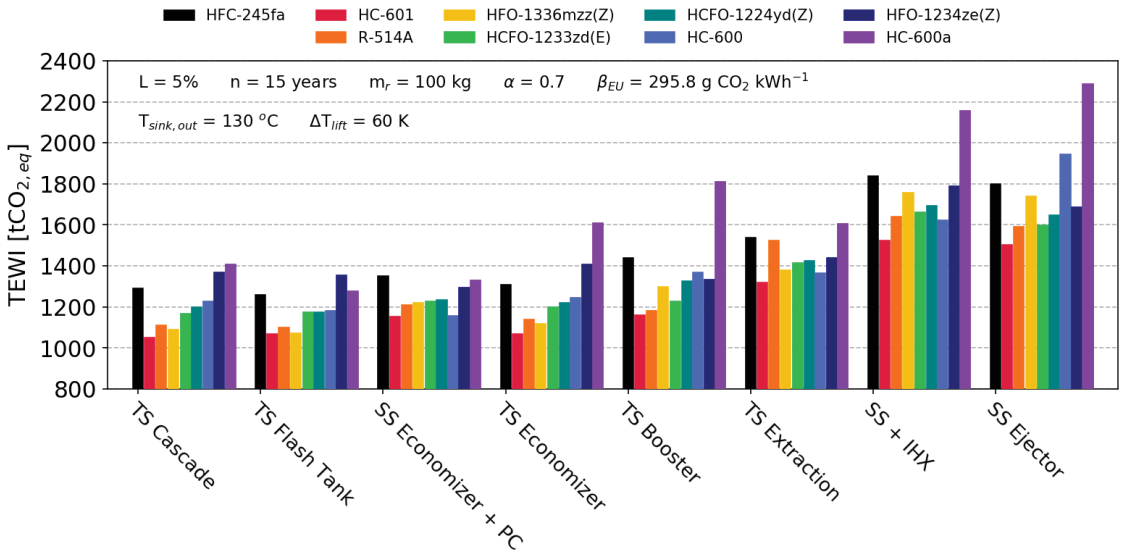

Fig. 18. Environmental analysis through the TEWI metric of each configuration and refrigerant

5. Conclusions

This work comprehensively evaluates advanced HTHP configurations for industrial waste heat recovery using low GWP refrigerants. The aim is to investigate the most promising configurations and refrigerants from energy, economic, and environmental perspectives to illustrate efficient and innovative solutions that contribute to climate change mitigation. The following conclusions are extracted:

- The selection of the configuration becomes highly dependent on the temperature lift and the application. For low-temperature lifts (below 50 K), single compression stage configurations are more convenient, whereas two-stage compression cycles exhibit significant potential at high temperature lifts (60 K and above).

- The highest COP improvement is obtained by the TS Cascade cycle, around 15% compared to the reference (TS Economizer), when using low-grade waste heat temperature sources (high temperature lifts). For high-grade waste heat temperature sources (low temperature lifts) and using HFC-245fa, the SS Economizer + PC becomes the most appropriate configuration obtaining a COP and VHC improvement up to 5% and 86%, respectively, compared with the reference cycle.

- The highest COP improvements are observed using the refrigerants HC-601, HFO-1336mzz(Z), and R-514A, which also show the lowest VHC values. On the contrary, HC-600 and HC-600a present the highest VHC values with slight COP improvements or even significant performance drop, respectively. HCFO-1233zd(E) and HCFO-1224yd(Z) show a compromise between COP and VHC. The refrigerant selection will be determined by the energy and installation cost for each application.

- The TS Booster cycle presents a significant potential for industrial waste heat recovery, for which two heat sources with different temperature levels are available. This configuration provides a COP and VHC improvement of 95% and 320%, respectively, compared to the reference cycle. Moreover, the TS Extraction cycle becomes an appropriate configuration to overcome the thermal demand of those industrial process that require a high heat sink glide. The COP and VHC increase are around 150% and 100%, respectively, compared to the TS Economizer (reference).

- The economic analysis illustrates a slight cost difference (around 9%) between the advanced configurations and reference TS Economizer cycle. Therefore, these configurations can be proposed as economically viable system solutions.

- The TEWI environmental analysis proves remarkable equivalent CO_2 emissions reduction, particularly for TS Cascade and SS Economizer + PC. Moreover, advanced HTHP configurations can reduce equivalent CO_2 emissions up to 68% compared to a natural gas boiler as a conventional heating system.

Acknowledgements

This research project is part of the Swiss Competence Center for Energy Research SCCER EIP of the Swiss Innovation Agency Innosuisse. The authors acknowledge the Spanish Government for the financial support under project RTC-2017-6511-3. Furthermore, the authors acknowledge the Universitat Jaume I (Castelló de la Plana, Spain) for the financial support under the projects UJI-B2018-24 and Carlos Mateu-Royo for the funding received through the PhD grant PREDOC/2017/41. Adrián Mota-Babiloni acknowledges the financial support of the Valencian Government under the postdoctoral contract APOSTD/2020/032.

References

[1] Bergamini R, Jensen JK, Elmegaard B. Thermodynamic competitiveness of high temperature vapor compression heat pumps for boiler substitution. Energy 2019;182:110–21. doi:10.1016/J.ENERGY.2019.05.187.

[2] Arpagaus C, Bless F, Uhlmann M, Schiffmann J, Bertsch SS. High temperature heat pumps: Market overview, state of the art, research status, refrigerants, and application potentials. Energy 2018;152:985–1010. doi:10.1016/J.ENERGY.2018.03.166.

[3] Urbanucci L, Bruno JC, Testi D. Thermodynamic and economic analysis of the integration of high-temperature heat pumps in trigeneration systems. Appl Energy 2019;238:516–33. doi:10.1016/J.APENERGY.2019.01.115.

[4] Kosmadakis G. Estimating the potential of industrial (high-temperature) heat pumps for exploiting waste heat in EU industries. Appl Therm Eng 2019;156:287–98. doi:10.1016/J.APPLTHERMALENG.2019.04.082.

[5] Calm JM. The next generation of refrigerants - Historical review, considerations, and outlook. Int J Refrig 2008;31:1123–33. doi:10.1016/j.ijrefrig.2008.01.013.

[6] Patten KO, Wuebbles DJ. Atmospheric lifetimes and Ozone Depletion Potentials of trans-1-chloro-3,3,3-trifluoropropylene and trans-1,2-dichloroethylene in a three-dimensional model. Atmos Chem Phys 2010;10:10867–74. doi:10.5194/acp-10-10867-2010.

[7] AGC Chemicals. AMOLEA® 1224yd, Technical Information, ASAHI Glass Co., Ltd.

2017:1–18.

[8] BAFU. Verordnung zur Reduktion von Risiken beim Umgang mit bestimmten besonders gefährlichen Stoffen, Zubereitungen und Gegenständen (Chemikalien-Risikoreduktions-Verordnung) (ChemRRV), Stand 9. Juli 2019. vol. 814.81. 2019.

[9] Kontomaris K. Zero-ODP, Low-GWP, Nonflammable Working Fluids for High Temperature Heat Pumps. ASHRAE Annu Conf Seattle, Washington, July 1, 2014 2014:1–40.

[10] Juhasz JR. Novel Working Fluid , HFO-1336mzz (E), for Use in Waste Heat Recovery Application. 12th IEA Heat Pump Conf 2017, Rotterdam 2017.

[11] Fukuda S, Kondou C, Takata N, Koyama S. Thermodynamic Analysis on High Temperature Heat Pump cycles using Low-GWP refrigerants for Heat recovery. 12th IEA Heat Pump Conf 2017, Rotterdam 2017:1–7.

[12] Fukuda S, Kondou C, Takata N, Koyama S. Low GWP refrigerants R1234ze(E) and R1234ze(Z) for high temperature heat pumps. Int J Refrig 2014;40:161–73. doi:10.1016/j.ijrefrig.2013.10.014.

[13] Kondou C, Koyama S. Thermodynamic Assessment of High-Temperature Heat Pumps for Heat Recovery. 15th Int. Refrig. Air Cond. Conf. Purdue, July 14-17, 2014, 2014, p. 1–10.

[14] Hu B, Wu D, Wang LW, Wang RZ. Exergy analysis of R1234ze(Z) as high temperature heat pump working fluid with multi-stage compression. Front Energy 2017:1–10.

[15] Arpagaus C, Prinzing M, Kuster R, Bless F, Uhlmann M, Schiffmann J, et al. High temperature heat pumps -Theoretical study on low GWP HFO and HCFO refrigerants. ICR 2019, 25th IIR Int. Congr. Refrig. August 24-30, Montréal, Québec, Canada, 2019, p. 1–8. doi:10.18462/iir.icr.2019.259.

[16] Helminger F, Kontomaris K, Pfaffl J, Hartl M, Fleckl T. Measured Performance of a High Temperature Heat Pump with HFO-1336mzz-Z as the Working Fluid. ASHRAE 2016 Annu. Conf. St. Louis, Missouri, 25-29 June 2016, 2016, p. 1–8.

[17] Nilsson M, Risla HN, Kontomaris K. Measured performance of a novel high temperature heat pump with HFO-1336mzz-Z as the working fluid. 12th IEA Heat Pump Conf. 2017, Rotterdam, 2017, p. 1–10.

[18] Frate GF, Ferrari L, Desideri U. Analysis of suitability ranges of high temperature heat pump working fluids. Appl Therm Eng 2019;150:628–40. doi:10.1016/J.APPLTHERMALENG.2019.01.034.

[19] Mateu-Royo C, Navarro-Esbrí J, Mota-Babiloni A, Amat-Albuixech M, Molés F. Theoretical evaluation of different high-temperature heat pump configurations for low-grade waste heat recovery. Int J Refrig 2018. doi:10.1016/j.ijrefrig.2018.04.017.

[20] Bamigbetan O, Eikevik TM, Nekså P, Bantle M, Schlemminger C. Theoretical analysis of suitable fluids for high temperature heat pumps up to 125 °C heat delivery. Int J Refrig 2018;92:185–95. doi:10.1016/j.ijrefrig.2018.05.017.

[21] Mota-Babiloni A, Mateu-Royo C, Navarro-Esbrí J, Molés F, Amat-Albuixech M, Barragán-Cervera Á. Optimisation of high-temperature heat pump cascades with internal

heat exchangers using refrigerants with low global warming potential. Energy 2018;165:1248–58. doi:10.1016/j.energy.2018.09.188.

[22] Mateu-Royo C, Navarro-Esbrí J, Mota-Babiloni A, Amat-Albuixech M, Molés F. Thermodynamic analysis of low GWP alternatives to HFC-245fa in high-temperature heat pumps: HCFO-1224yd(Z), HCFO-1233zd(E) and HFO-1336mzz(Z). Appl Therm Eng 2019. doi:10.1016/j.applthermaleng.2019.02.047.

[23] Luo B, Zou P. Performance analysis of different single stage advanced vapor compression cycles and refrigerants for high temperature heat pumps. Int J Refrig 2019;104:246–58. doi:https://doi.org/10.1016/j.ijrefrig.2019.05.024.

[24] Alhamid MI, Aisyah N, Nasruddin N, Lubis A. Thermodynamic and Environmental Analysis of a High-temperature Heat Pump using HCFO-1224yd(Z) and HCFO-1233zd(E). Int J Technol 2019;10:1585. doi:10.14716/ijtech.v10i8.3459.

[25] Mikielewicz D, Wajs J. Performance of the very high-temperature heat pump with low GWP working fluids. Energy 2019;182:460–70. doi:10.1016/j.energy.2019.05.203.

[26] Wu D, Hu B, Wang RZ, Fan H, Wang R. The performance comparison of high temperature heat pump among R718 and other refrigerants. Renew Energy 2020;154:715–22. doi:10.1016/j.renene.2020.03.034.

[27] Bai T, Yan G, Yu J. Thermodynamic assessment of a condenser outlet split ejector-based high temperature heat pump cycle using various low GWP refrigerants. Energy 2019;179:850–62. doi:10.1016/J.ENERGY.2019.04.191.

[28] Mateu-Royo C, Sawalha S, Mota-Babiloni A, Navarro-Esbrí J. High temperature heat pump integration into district heating network. Energy Convers Manag 2020;210:112719. doi:10.1016/J.ENCONMAN.2020.112719.

[29] Diewald K, Arpagaus C, Hebenstreit B. Thermodynamic analysis of low GWP HFO and HCFO refrigerants in HTHP with large temperature glides on the heat sink. IIR Int. Rank. 2020 Conf. – Heating, Cool. Power Gener. – 26-29 July 2020, Glas. UK, 2020, p. 1–8. doi:10.18462/iir.rankine.2020.1166.

[30] Arpagaus C, Kuster R, Prinzing M, Bless F, Uhlmann M, Büchel E, et al. High temperature heat pump using HFO and HCFO refrigerants - System design and experimental results. 25th IIR Int. Congr. Refrig. (ICR 2019). Montréal, Québec, Canada., 2019. doi:10.18462/iir.icr.2019.242.

[31] Kondou C, Koyama S. Thermodynamic assessment of high-temperature heat pumps using low-GWP HFO refrigerants for heat recovery. Int J Refrig 2015;53:126–41. doi:10.1016/j.ijrefrig.2014.09.018.

[32] Zhang Z, Feng X, Tian D, Yang J, Chang L. Progress in ejector-expansion vapor compression refrigeration and heat pump systems. Energy Convers Manag 2020;207:112529. doi:https://doi.org/10.1016/j.enconman.2020.112529.

[33] Chahla GABI, Beucher Y, Zoughaib A, De Carlan F, Pierucci J. Transcritical industrial heat pump using HFO's for up to 150°C hot air supply. ICR 2019, August 24-30, Montréal, Canada, 2019, p. 1–8. doi:10.18462/iir.icr.2019.1184.

[34] Sarkar J, Agrawal N. Performance optimization of transcritical CO2 cycle with parallel compression economization. Int J Therm Sci 2010;49:838–43.

doi:10.1016/j.ijthermalsci.2009.12.001.

[35] Yu B, Yang J, Wang D, Shi J, Chen J. An updated review of recent advances on modified technologies in transcritical CO2 refrigeration cycle. Energy 2019;189:116147. doi:10.1016/j.energy.2019.116147.

[36] Arpagaus C, Bless F, Schiffmann J, Bertsch SS. Multi-temperature heat pumps: A literature review. Int J Refrig 2016;69. doi:10.1016/j.ijrefrig.2016.05.014.

[37] Klein S. Engineering Equation Solver (EES) V10.6. Fchart Software, Madison, USA WwwFchartCom 2006.

[38] ASHRAE. ASHRAE Handbook Fundamentals. Am Soc Heating, Refrig Air-Conditioning Eng 2017.

[39] Lemmon EW, Bell IH, Huber ML, McLinden MO. NIST Standard Reference Database: Reference Fluid Thermodynamic and Transport Properties-REFPROP, Version 10. Natl Inst Stand Technol Stand Ref Data Program, Boulder, CO 2018.

[40] Hoang AT. Waste heat recovery from diesel engines based on Organic Rankine Cycle. Appl Energy 2018;231:138–66. doi:10.1016/J.APENERGY.2018.09.022.

[41] Hammond GP, Norman JB. Heat recovery opportunities in UK industry. Appl Energy 2014;116:387–97. doi:10.1016/j.apenergy.2013.11.008.

[42] Winandy E, Saavedra O C, Lebrun J. Simplified modelling of an open-type reciprocating compressor. Int J Therm Sci 2002;41:183–92. doi:10.1016/S1290-0729(01)01296-0.

[43] Cuevas C, Lebrun J, Lemort V, Winandy E. Characterization of a scroll compressor under extended operating conditions. Appl Therm Eng 2010;30:605–15. doi:10.1016/J.APPLTHERMALENG.2009.11.005.

[44] Lemort V, Quoilin S, Cuevas C, Lebrun J. Testing and modeling a scroll expander integrated into an Organic Rankine Cycle. Appl Therm Eng 2009;29:3094–102. doi:10.1016/J.APPLTHERMALENG.2009.04.013.

[45] Tello-Oquendo FM, Navarro-Peris E, Barceló-Ruescas F, Gonzálvez-Maciá J. Semi-empirical model of scroll compressors and its extension to describe vapor-injection compressors. Model description and experimental validation. Int J Refrig 2019;106:308–26. doi:https://doi.org/10.1016/j.ijrefrig.2019.06.031.

[46] Cui Z, Qian S, Yu J. Performance assessment of an ejector enhanced dual temperature refrigeration cycle for domestic refrigerator application. Appl Therm Eng 2020. doi:10.1016/j.applthermaleng.2019.114826.

[47] He S, Li Y, Wang RZ. Progress of mathematical modeling on ejectors. Renew Sustain Energy Rev 2009;13:1760–80. doi:10.1016/J.RSER.2008.09.032.

[48] Makhnatch P, Khodabandeh R. The role of environmental metrics (GWP, TEWI, LCCP) in the selection of low GWP refrigerant. Energy Procedia 2014;61:2460–3. doi:10.1016/j.egypro.2014.12.023.

[49] IPCC. IPCC/TEAP special report on safeguarding the ozone layer and the global climate system: Issues related to hydrofluorocarbons and perfluorocarbons. Cambridge Publ Intergov Panel Clim Chang [by] Cambridge Univ Press 2005.

[50] EEA. Overview of electricity production and use in Europe. Eur Enviroment Agency 2018.

[51] Fang Z, Fan C, Yan G, Yu J. Performance evaluation of a modified refrigeration cycle with parallel compression for refrigerator-freezer applications. Energy 2019;188:116093. doi:https://doi.org/10.1016/j.energy.2019.116093.

[52] Scoccia R, Toppi T, Aprile M, Motta M. Absorption and compression heat pump systems for space heating and DHW in European buildings: Energy, environmental and economic analysis. J Build Eng 2018;16:94–105. doi:10.1016/J.JOBE.2017.12.006.